

UCLA

UCLA Electronic Theses and Dissertations

Title

Biomimetic hydroxyapatite as a new consolidating agent for archaeological bone

Permalink

<https://escholarship.org/uc/item/6tq8k3zh>

Author

North, Alexis

Publication Date

2014

Peer reviewed|Thesis/dissertation

UNIVERSITY OF CALIFORNIA

Los Angeles

Biomimetic hydroxyapatite as a new consolidating agent for archaeological bone

A thesis submitted in partial satisfaction

of the requirements for the degree Master of Arts

in Conservation of Archaeological and Ethnographic Materials

by

Alexis E. North

2014

ABSTRACT OF THE THESIS

Biomimetic hydroxyapatite as a new consolidating agent for archaeological bone

by

Alexis E. North

Master of Arts in Conservation of Archaeological and Ethnographic Materials

University of California, Los Angeles, 2014

Professor Ioanna Kakoulli, Chair

Recent studies on calcareous stone and plaster consolidation have demonstrated considerable potential by bio-mimicking the growth of hydroxyapatite (HAP), the main mineralogical constituent of teeth and bone matrix. These initial conservation applications, together with significant fundamental research on the precipitation of HAP for bioengineering and biomedical applications, offer great promise in the use of HAP as a consolidating agent for archaeological bone and other similar materials such as archaeological teeth, ivory, and antler. Experimental research via the controlled application of diammonium phosphate (DAP) precursors to bone flour, modern bone samples, and archaeological bones, indicated the *in situ* formation of HAP

with a simultaneous increase in the cohesiveness of friable bone material, while preserving the bone's physiochemical properties. These preliminary results point towards a promising new method in archaeological conservation.

The thesis of Alexis E. North is approved.

Christian Fischer

Benjamin Wu

Magdalena Balonis-Sant

Ioanna Kakoulli, Committee Chair

University of California, Los Angeles
2014

Table of Contents

Chapter 1: Introduction	1
1.1 Scope of research	3
Chapter 2: Biomimetic hydroxyapatite as a consolidating agent for stone and plaster	4
Chapter 3: Bone chemistry, properties and deterioration	6
3.1 Physical structure and chemical properties of bone	6
3.2 Chemical composition and physical properties of apatite minerals	8
3.3 Diagenesis of archaeological bone and its impact on archaeology and conservation	10
Chapter 4: Bone consolidation literature review	14
4.1 Traditional bone consolidating agents and methods	14
Chapter 5: Materials and methods.....	16
5.1 Materials	17
5.1.1 Substrates: bone flour, modern and archaeological bone.....	17
5.1.2 Consolidants tested	17
5.2 Application methodology	19
5.2.1 Application of consolidants on the bone flour samples.....	19

5.2.2	<i>Application of organic consolidants and DAP precursor on modern and archaeological bone samples</i>	21
5.3	Characterization methods.....	22
5.3.1	<i>Digital microscopy (DM)</i>	22
5.3.2	<i>Scanning electron microscopy (SEM) and energy dispersive X-ray spectroscopy (EDS)</i>	22
5.3.3	<i>X-ray diffraction (XRD)</i>	23
5.3.4	<i>Water drop absorption</i>	23
Chapter 6: Results		24
6.1	Surface wettability and water drop absorption	25
6.1.1	<i>Consolidation effect and water drop absorption on bone flour samples</i>	25
6.1.2	<i>Water drop absorption of modern bone samples</i>	29
6.1.3	<i>Water drop absorption of archaeological bone samples</i>	31
6.2	Digital (DM) and scanning electron microscopy (SEM)	32
6.2.1	<i>Modern bones samples</i>	32
6.3	Archaeological bone samples.....	36
Chapter 7: Discussion		39

7.1	Surface wettability and sorptivity	39
7.2	Surface topography and porosity	40
7.3	Reaction chemistries	40
7.3.1	<i>Magnesium ammonium phosphate (struvite) formation</i>	40
7.3.2	<i>Amorphous calcium phosphate</i>	43
7.3.3	<i>Calcium-deficient phosphate phases</i>	45
Chapter 8: Conclusions		48
8.1	Further Research	49
8.1.1	<i>Future experimental and theoretical testing</i>	49
8.1.2	<i>Use on teeth and ivory</i>	49
8.1.3	<i>Effects on paleodietary and other analyses</i>	50
8.1.4	<i>Additional calcium sources</i>	50
Chapter 9: Appendix		52
9.1	Time frame for use of various consolidants on bone and fossil, for the time period 1900-1985 (based on Howie 1984 and Johnson 1994)	52
9.2	XRD spectrum of bone flour sample	53

9.3	Analysis of poultice used on archaeological bone samples	54
9.3.1	<i>XRF spectrum of poultice</i>	54
9.3.2	<i>XRD spectrum of poultice</i>	55
9.4	XRD spectra of bone flour samples after treatment with DAP	56
9.4.1	<i>Sample treated with 0.5M DAP</i>	56
9.4.2	<i>Sample treated with 1.0M DAP</i>	57
9.4.3	<i>Sample treated with 2.0M DAP</i>	58
9.5	Digital Microscope photomicrographs of modern bone samples	59
9.5.1	<i>DM images of modern bone treated with 1.0M DAP, revealing crystals on the surface and their largest dimension</i>	59
9.6	SEM-EDS of bone flour samples	60
9.7	SEM-EDS of modern bone samples	62
9.7.1	<i>Sample treated with 0.5M DAP</i>	62
9.7.2	<i>Sample treated with 1.0M DAP</i>	63
9.8	EDS of archaeological bone samples.....	65
Chapter 10: References		69

Table of Figures

Figure 1. SEM image of HAP formed between limestone grains. The stone was treated with 1M DAP (diammonium hydrogen phosphate) for 2 days before imaging. From Sassoni, Naidu, and Scherer 2011.....	5
Figure 2. Illustration of the basic composition and growth of a generic long bone, from Mays 2010.....	7
Figure 3. Molecular structure of the unit cell of HAP, looking down at the basal plane. Adapted from Eanes and Posner 1970.....	9
Figure 4. SEM image of an archaeological bone cross-section, showing a) radial cracks, b) circumferential cracks, c) bacterial alteration, and d) Haversian canal filled with carbonate material. From Rogoz, Sawlowicz, and Wojtal 2012.	12
Figure 5. Silicone mold with bone flour samples, after testing. Column A was consolidated with 0.5M DAP, column B with 1.0M DAP, and column C with 2.0M DAP. In addition, 2B and 3B received one drops of ethanol prior to consolidation, while 2C and 3C received two drops of ethanol, to improve the wetting and penetration of the consolidant.	20
Figure 6A. Results illustrating the water absorption time in seconds of the mean values (N=6 for each) of tests A1-A3, B1-B3, and C1-C3 using 0.5M, 1.0M and 2.0M DAP solutions (see table in Figure 5) on bone flour samples. Reference water absorption time=4s.	26

Figure 6B. Results illustrating the water absorption (WA) % – normalized to the absorption of the reference/untreated sample – of the mean values (N=6 for each) of tests A1-A3, B1-B3, and C1-C3 using 0.5M, 1.0M and 2.0M DAP solutions (see table in Figure 5) performed on bone flour samples. Reference water absorption time=4s.26

Figure 7. Photomicrographs of bone flour samples impregnated with blue colored resin. A-B: 0.5M, C-D: 1.0M, E-F: 2.0M treated samples. Photomicrographs B, D, and F are higher magnifications of photomicrographs A, C, and E.28

Figure 8. Bone flour sample treated with 3% B-72, which broke upon trying to remove it from its silicone mold. Pigmented B-72 was used in an attempt to better visualize the consolidant penetration via cross-sectioning, but the lack of consolidation to the sample made this impossible.....29

Figure 9A. Results of water absorption tests on modern bone samples treated with 0.5 and 1.0 M DAP solutions respectively before (reference sample) and after treatment (mean N=3). As it can be seen from the graph there is a change in wettability of the surface resulting in reduced absorption times of the treated areas, especially for the 1.0M DAP treated area.30

Figure 9B. Results illustrating the water absorption (WA) % – normalized to the absorption of the reference/untreated sample – of the mean values (N=3 for each) of tests using 1.0 and 0.5 M DAP solutions. Considering that the absorption of the reference untreated surface is

set equal to 100% the high increase especially for 1.0M indicates a change of the surface wettability and an unexpected anomaly in the measurements.41

Figure 10A. Results of water absorption tests on archaeological bone samples (Arch 1 and Arch 2) treated with 1.0 M DAP solution before (reference sample) and after treatment on both sides of each sample: side A (surface in contact with the poultice) and side B (back surface away from the poultice). As it can be seen from the graph there is a slight change in wettability of the surface in sample Arch 1, side B resulting in reduced absorption time...31

Figure 10B. Mean values (N=4) of water absorption (WA%) for the archaeological samples treated with 1.0M DAP measured on two sides of the bone: side A (surface in contact with the poultice) and side B (back surface away from the poultice).43

Figure 11. DM and SEM photomicrographs of the reference sample (A and C) and sample treated with Acrysol WS-24, with B and D clearly showing the difference in surface porosity and topography after treatment. After treatment the texture of the surface shows a glossy finish (B) and the pores (C) are clearly filled with the consolidant (D).....33

Figure 12. DM and SEM photomicrographs of the reference sample (A and C) and treated with Paraloid B-72, with B and D clearly showing noticeable differences in surface porosity and topography after treatment. After treatment, the texture of the surface shows a glossy finish (B) and the pores (C) are clearly filled with the consolidant (D).....34

Figure 13. DM (A-B) and SEM (C-D) micrographs of crystals formed on the surface of both the 1.0M (A and C) and 0.5M (B and D) treated modern bone samples.35

Figure 14. SEM micrograph (left) and EDS spectrum of the orthorhombic crystal found on the modern bone treated with 1.0M DAP. The white circle on the SEM image shows the location of the EDS spot measurement.36

Figure 15. SEM micrographs of the surface of an archaeological bone sample (A) and modern bone (B) both treated with 1.0M DAP. Surface crystals found on the modern bones are many times larger than those found on the archaeological samples (indicated by the arrows).37

Figure 16. SEM-EDS micrograph and EDS spectra revealing the elemental composition of the magnesium phosphate (1) orthorhombic-like crystal, needle-like calcium-deficient calcium phosphate crystals (2), and original bone surface (3).38

Figure 17a-b. SEM image of 2.0M treated bone flour sample. The area within the red circle resembles hexagonal plate-like crystals of HAP, but this could not be confirmed by other analytical methods.45

Figure 18. SEM photomicrograph of archaeological bone sample after treatment, showing both magnesium phosphate (blue arrows) and calcium-deficient calcium phosphate (red arrows) formations on the sample’s surface.47

Chapter 1: Introduction

Consolidation, in conservation terms, is broadly defined as the process of reestablishing the loss of matrix cohesion at the microscopic scale and providing mechanical integrity. It is one of the most crucial treatments in conservation practice as it is not an easily reversible operation. Consolidating agents need to provide stability, cohesion and strength; limit water ingress; and be easy to use, non-toxic and stable over time. They should also remain unaltered in the presence of soluble salts, which are often found in burial sites, and resistant to weathering and other deterioration factors.

Commonly in archaeological conservation, synthetic polymers such as acrylics are used at different concentrations and application methods. However, their use on porous archaeological materials could be detrimental, limiting the potential of the artifact to be retreatable. Inorganic precursors including calcium hydroxide ($\text{Ca}(\text{OH})_2$) both as dispersions and colloids (Baglioni and Giorgi 2006; Chelazzi et al. 2013; Hansen et al. 2003; Warren 1999), barium hydroxide ($\text{Ba}(\text{OH})_2$) and oxalate salts (such as ammonium oxalate- $(\text{NH}_4)_2\text{C}_2\text{O}_4$) (Matteini 2003; Matteini 2010), have been tested and used as alternatives to organic polymer-based reagents for the consolidation of porous materials. While these provided effective cohesion of powdery matrices based on mineralization processes, there are some limiting factors in their use caused by their instability at variable pH (mainly in the use of $\text{Ca}(\text{OH})_2$ precursor); toxicity (in the case of $\text{Ba}(\text{OH})_2$); and the random formation of coherent 'layers' due to incompatibility of crystal structure and poor penetration (using $(\text{NH}_4)_2\text{C}_2\text{O}_4$).

Recent studies, mainly on stone consolidation (Matteini 2010; Sassoni, Naidu, and Scherer 2011; Yang et al. 2011), have demonstrated considerable potential for developing improved consolidation efficiency, providing rigidity and strength by bio-mimicking the growth of hydroxyapatite (HAP), the main mineralogical constituent of teeth and bone matrix with the general formula $\text{Ca}_{10}(\text{PO}_4)_6\text{X}_2$, with X usually representing fluorine (fluorapatite), hydroxyl (hydroxy- or hydroxylapatite), or chlorine (chlorapatite) (Brown and Constantz 1994; Posner 1969; Serbetci, Korkusuz, and Hasirci 2000; Wilson, Elliott, and Dowker 1999). In addition to restoring the mechanical integrity of weathered stones (Sassoni, Naidu, and Scherer 2011), HAP has also demonstrated protective properties, as it was identified on “well-preserved” old carbonate stones and walls that have been in contact with a phosphate-rich environment (Polikreti and Maniatis 2003; Sassoni, Naidu, and Scherer 2011). These preliminary conservation science applications, together with significant fundamental research on the precipitation of HAP for bioengineering and biomedical applications for teeth reconstruction and bone regeneration, offer great promise in the use of HAP as a consolidating agent for archaeological bone and other similar materials such as archaeological teeth, ivory, and antler.

In light of this evidence, this research exploits the aforementioned advances in bioengineering and conservation science to develop hydroxyapatite consolidation treatments through remineralization reactions between phosphate precursors and archaeological bone. As such, the critical questions that need to be answered for the successful execution of this method from a scientific and practical perspective are:

- How can ‘biomimetic’ hydroxyapatite crystals with suitable consolidating properties be precipitated in a controlled fashion within disintegrated/decohesive bone matrices and

other mineralized calcium-rich archaeological materials to improve cohesion, stability and strength in relation to the substrate and precursor reactant characteristics?

- How can we design, engineer and optimize the physical and chemical properties of the reactant formulation and the application strategy to achieve the desired consolidation response?

To better answer these questions, this research seeks to develop a unified, context-sensitive approach for consolidation treatments applicable to fragile bone and calcified bio-archaeological materials.

1.1 Scope of research

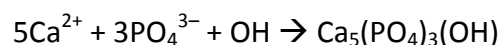
This research builds upon the biomimetic synthesis concept to induce the growth of HAP on calcium-rich mineral surfaces for consolidation purposes. The reaction for the formation of HAP is based on the introduction of soluble phosphate precursors that can react with the calcium of the bone to induce *in situ* HAP mineralization.

In this research I examine the use of biomimetic HAP growth within the bone matrix in regards to its behavior, degree of consolidation, and suitability as a conservation material. Following this introduction (Chapter 1), Chapter 2 outlines the use of HAP remineralization as a consolidation mechanism for stone and plaster. Chapter 3 provides an assessment of the physical and chemical properties of bone and its diagenetic alterations. Chapter 4 offers a systematic review of past and present bone consolidation methods. Chapter 5 describes the materials, application methods, and analytical techniques used to test HAP as a suitable

consolidant, and Chapter 6 presents the results. Chapter 7 discusses the findings and Chapter 8 concludes with an examination of drawbacks, further ideas and future research.

Chapter 2: Biomimetic hydroxyapatite as a consolidating agent for stone and plaster

Recent experiments using hydroxyapatite as a consolidating agent on weathered stones have shown significant improved cohesiveness and overall structural stability of the stone. Samples consolidated with HAP have shown an increase in elastic and tensile strength, and reduction in micro-cracks (Sassoni, Naidu, and Scherer 2011). For the formation of HAP, a phosphate solution, either monoammonium (MAP) or diammonium phosphate, also known as diammonium hydrogen phosphate (DAP), with chemical formula $(\text{NH}_4)_2\text{HPO}_4$, is applied by brush, injection or spraying. Some experiments were also conducted by total immersion of the samples into the solution (Matteini et al. 2011; Sassoni, Naidu, and Scherer 2011; Yang et al. 2011). The transformation/precipitation reaction then forms a HAP network between the calcium in the stone and the phosphate solutions (Yang et al. 2011):



HAP has a crystal structure very similar to that of calcite, enabling epitaxial growth over calcareous matrices (Sassoni, Naidu, and Scherer 2011). *In situ* scanning electron microscopy (SEM) and energy-dispersive x-ray spectroscopy (EDS) was used to study the morphology and growth of HAP, confirming its precipitation inside the inner surface of pores and at the grain boundaries of the stone samples (Figure 1). Through the identification of nitrogen, it was also

possible to monitor the presence of residual ammonium inside the samples (Sassoni, Naidu, and Scherer 2011).

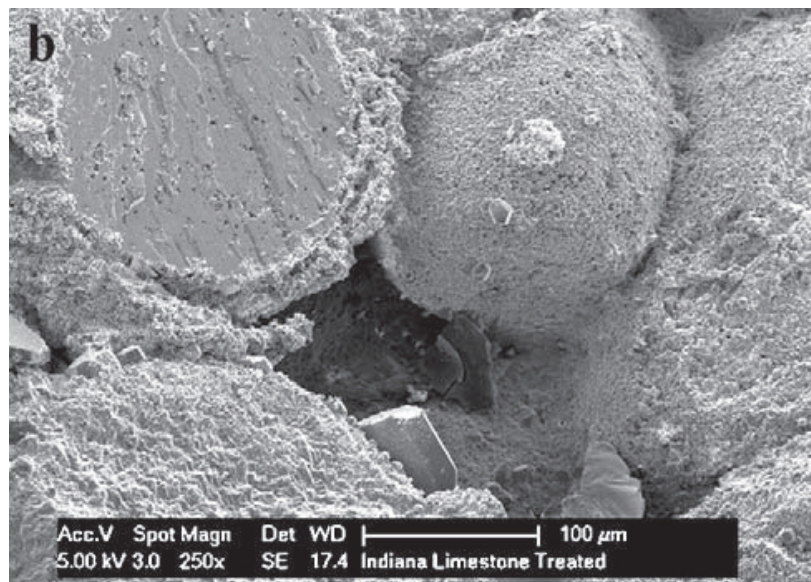


Figure 1. SEM image of HAP formed between limestone grains. The stone was treated with 1M DAP (diammonium hydrogen phosphate) for 2 days before imaging. From Sassoni, Naidu, and Scherer 2011.

Calcium content can also be introduced or increased, through pre-treatment with a nano-calcium hydroxide /alcohol dispersion. The particles of the calcium hydroxide/alcohol dispersion fill larger gaps and cavities and upon exposure to atmospheric CO₂ they convert into calcium carbonate. In experiments using calcium hydroxide/alcohol dispersions and ammonium phosphate with calcareous stones, SEM analysis revealed that HAP coats the newly formed calcium carbonate deposition, without consuming it completely. However, there was still a significant positive change in the strength of the stone samples (Yang et al. 2011). It is important to remember that this is not an immediate process. A successful HAP network was grown within stone only after about two weeks, but during that time the material would still be

weak and friable. For large stone structures, this time delay is less important than when treating small finds in active excavations. However, the apparent success of this treatment may outweigh the delay it would cause to post-excavation study and analysis.

Chapter 3: Bone chemistry, properties and deterioration

3.1 Physical structure and chemical properties of bone

The skeleton of most animals consists of three types of bone: long bones, flat bones, and irregular bones. These are made of two types of bone growth, cortical (or compact), and cancellous (or trabecular) bone (Eanes and Posner 1970). Cortical bone is the solid, dense outer layer of bone, which belies an expansive network of microscopic channels, called Haversian canals, which run along the length of the bone, and Volkmann canals, which run perpendicular and connect to the Haversian canals. These canals allow for blood vessels to run through the bone and provide nourishment. Around each of the Haversian canals, the bone develops a cylindrical structure known as an osteon, consisting of thin concentric layers of compact bone tissue or lamellae (Figure 2). Additional lamellae, called interstitial lamellae, exist between the osteons (Mays 2010). Cancellous bone is less dense than cortical bone, with a honeycomb structure that helps dissipate the mechanical stresses at the joints. Cancellous bone has blood vessels running throughout its open structure, and so it lacks a Haversian system (Mays 2010).

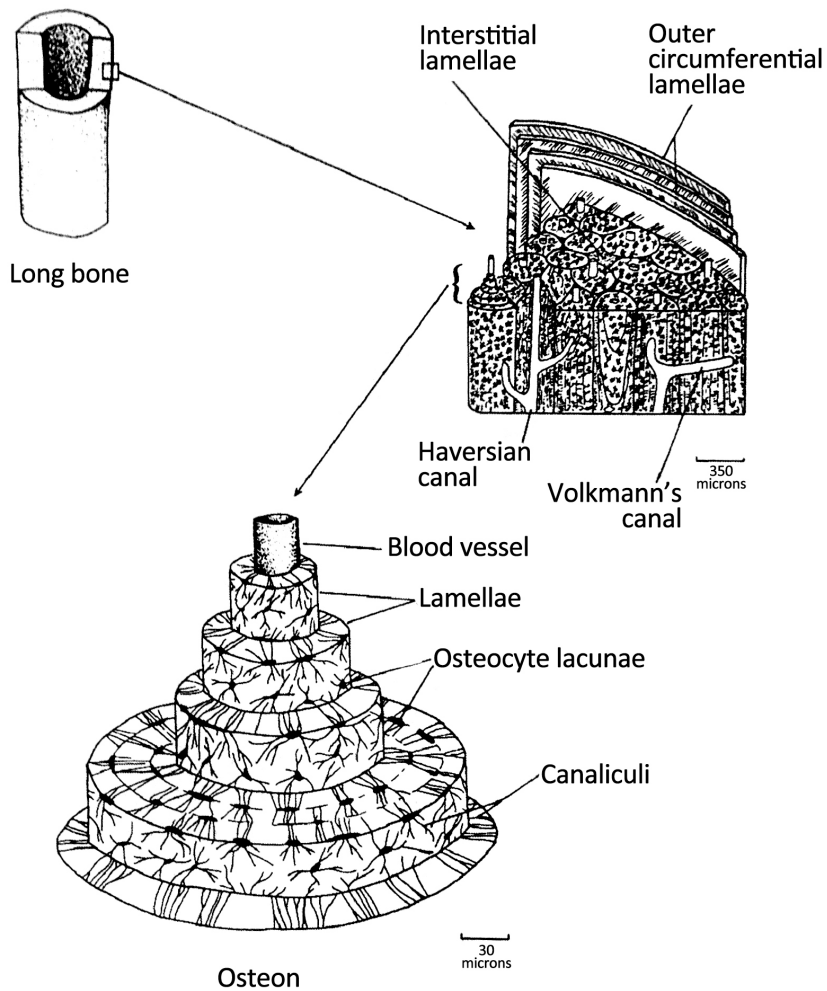


Figure 2. Illustration of the basic composition and growth of a generic long bone, from Mays 2010.

Chemically, bone is an extremely complex composite material, consisting of about 20-30 wt% collagen, 60-70 wt% minerals, and 10 wt% water (Reiche, Vignaud, and Menu 2002). The mineral content is made primarily of carbonated hydroxyapatite, with varying lesser quantities of fluorine, sodium, magnesium, and strontium substituting for calcium, hydroxyl, or phosphate. Other elements, such as silicon, manganese, and iron can exist as independent mineral phases within microscopic cracks and voids (Eanes and Posner 1970; Parker and Toots

1970). XRD studies have shown that bone HAP crystals are very small; only a few hundred unit cells, in a sort of "mosaic of microcrystals" fused together, rather than well-developed single crystal structures (Eanes and Posner 1970).

3.2 Chemical composition and physical properties of apatite minerals

As stated earlier, the family of apatite minerals share the general chemical formula, $\text{Ca}_{10}(\text{PO}_4)_6\text{X}_2$, with X usually representing fluorine (fluorapatite), hydroxyl (hydroxy- or hydroxylapatite), or chlorine (chlorapatite). The apatite crystal structure tolerates many other substitutions, such as carbonate for X or phosphate and strontium and barium for calcium, as well as vacancies, creating a very large collection of similar, but not identical, chemical materials with varying physical properties (Eanes and Posner 1970; Elliott, Wilson, and Dowker 2002; Dorozhkin 2009).

The ideal crystallographic structure of HAP is monoclinic, however biologically derived HAP most often takes the shape of a right rhombic prism (Figure 3), which stacks together to form a hexagonal close-packed (HCP) lattice (Eanes and Posner 1970; Elliott, Wilson, and Dowker 2002; Suetsugu and Tanaka 2002; Dorozhkin 2009; Ma and Liu 2009), forming sheets arranged in an ABAB sequence, so that the first and third sheets, and second and fourth, etc., are aligned exactly over each other. (Elliott, Wilson, and Dowker 2002; Beevers and McIntyre 1946). Hydroxyl groups lie at the corners of the rhombic base, and align themselves in columns which run along the c-axis, perpendicular to the basal plane (Eanes and Posner 1970; Suetsugu and Tanaka 2002).

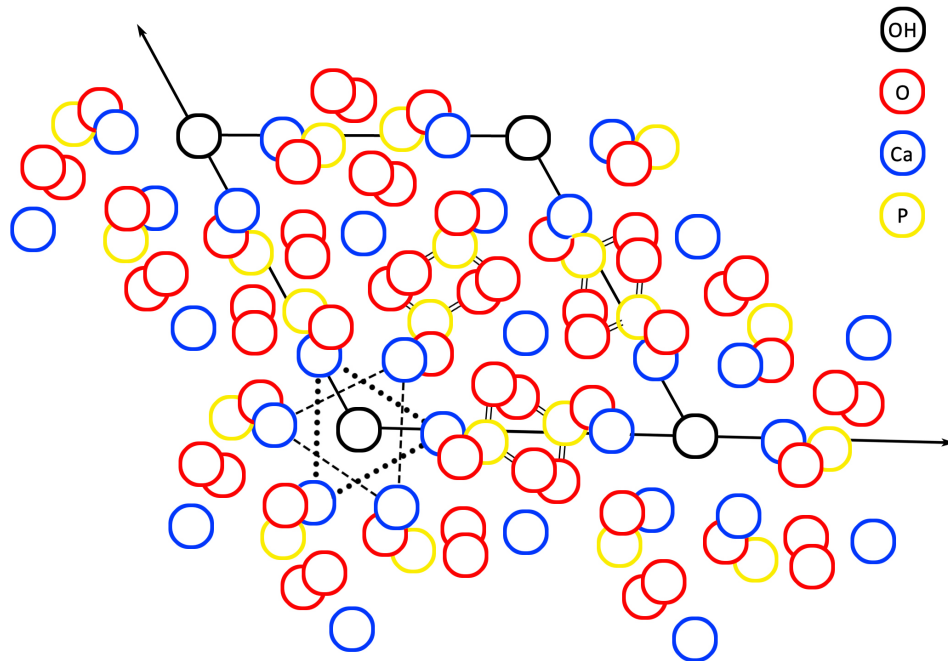


Figure 3. Molecular structure of the unit cell of HAP, looking down at the basal plane. Adapted from Eanes and Posner 1970.

Both organically derived and non-biogenetic HAP are formed through a two-step process, whereby amorphous calcium phosphate phases (such as octacalcium phosphate – OCP) which autocatalyze to form HAP crystals (Eanes and Posner 1968; Nancollas and Mohan 1970; Blumenthal and Posner 1973; Dorozhkin 2009; Sassoni, Naidu, and Scherer 2011).

This amorphous form exists in dense circular or oval rings (Eanes and Posner 1968). The percentage of amorphous HAP decreases over the lifetime of the individual, generally speaking from around 65 wt% at birth to 30 wt% of the total HAP content of the skeleton (Eanes, Termine, and Posner 1967; Blumenthal and Posner 1973). This correlates with diagenetic studies which show an increase in crystallinity of bone over time (Hedges 2002).

However, studies showing a total autocatalytic conversion of amorphous calcium phosphate into HAP in synthetic trials are contrary to what is known about the amorphous content in bone. While crystallinity increases slightly as an organism ages, that 30 wt% value means something is slowing or halting the conversion process (Eanes, Termine, and Posner 1967). The presence of magnesium is known to slow the process in laboratory conditions (Eanes, Termine, and Posner 1967; Eanes and Posner 1968; Tomazic, Tomson, and Nancollas 1975), but adult bone material has a very low magnesium content (Eanes, Termine, and Posner 1967; Freund et al. 2002). In actuality, the reason may be a combination of effects from the presence of magnesium, carbonates, polyelectrolyte anions and other organic components, or it may simply be that there is not enough free water to solubilize the amorphous calcium phosphate and allow it to convert into HAP (Eanes, Termine, and Posner 1967).

3.3 Diagenesis of archaeological bone and its impact on archaeology and conservation

The preservation of bone depends not on the length of time the bone has been underground, but the type of burial environment (Child 1995; Nielsen-Marsh and Hedges 2000; Hedges 2002). Alterations of buried bone are dependent on the decomposition of both the mineral and organic components. After deposition, bone can undergo ion exchange, loss of collagen, microbial attack, mineral leaching, and infiltration by organic or other mineral compounds found in the soil. Both the porosity and crystallinity of the bone affects how it continues to respond to the environment, and as the bone ages and degrades, the crystallinity changes even more (Hedges 2002).

Issues of wet/dry and freeze/thaw cycles, aggravated by soluble salts, can also add to the degradation of bone, as well as exposure to sunlight/ultraviolet (UV) radiation (Child 1995; Fernández-Jalvo et al. 2002). There are three major deterioration pathways for bone: 1) the chemical deterioration of collagen, 2) the chemical deterioration of mineral phases, and 3) biodegradation. The collagen and mineral contents of bone protect each other, as the presence of organics will slow mineral dissolution reactions, and conversely mineral dissolution can lead to an increase in the microbial degradation of collagen (Collins et al. 2002; Hedges 2002).

In general, alkaline soils will break down the collagen of bone, while preserving the mineral structure (Child 1995). However, highly alkaline soils can cause desquamation, or a peeling off of the bone surface in scaly fragments (Fernández-Jalvo et al. 2002). Acidic soils, with a pH of around 5 or lower, will dissolve the mineral structure of bone. HAP will also be lost if the burial soil is low in phosphates, leading to leaching of phosphate anions as the bone seeks equilibrium with the environment (Child 1995). It may also be transferred in solution some distance through the bone before being redeposited. In fact, it is possible for HAP crystals to dissolve and precipitate repeatedly in place (Hedges 2002). All of these events alter the crystallinity of the bone, possibly affecting its strength and long-term preservation after deposition. Once initial deterioration has occurred via chemical or physical means, microbiological action could also damage the bone, mostly by attacking the organic collagen component (Hedges 2002).

The dissolution of minerals is also more common in locations with water movement, where a large amount of ion transfer has to take place in order for the bone to come into

equilibrium with the aqueous environment (Collins et al. 2002; Hedges 2002). Bones from aqueous environments will be deprived of HAP, and therefore become more susceptible to subsequent deterioration of the collagen (Reiche, Vignaud, and Menu 2002). Soil high in calcium will also break up bone through calcite formation (Figure 4). The calcite crystals take up more volume within the bone's pores, causing cracking and flaking (Child 1995).

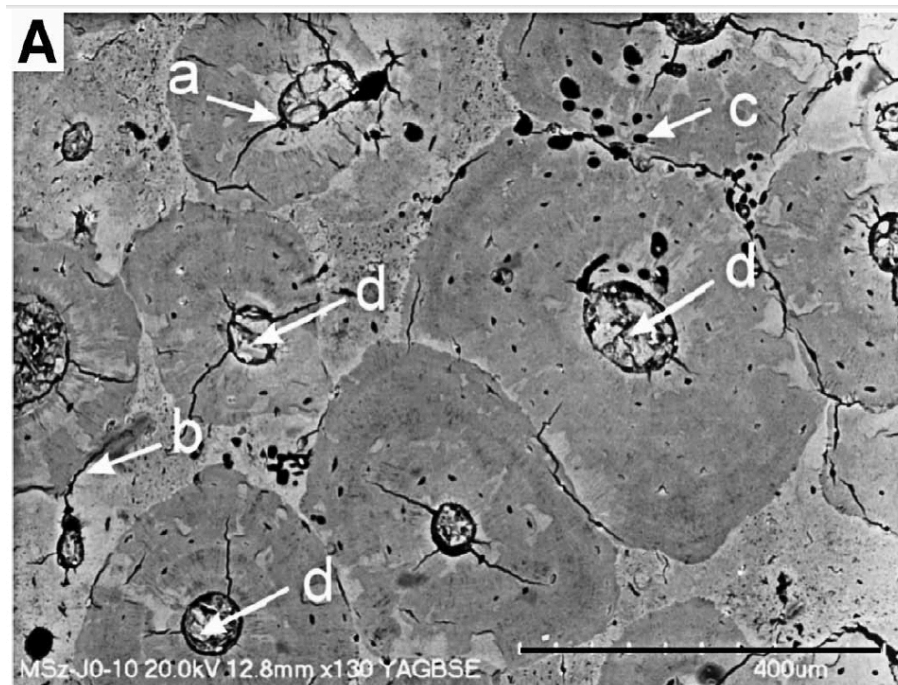


Figure 4. SEM image of an archaeological bone cross-section, showing a) radial cracks, b) circumferential cracks, c) bacterial alteration, and d) Haversian canal filled with carbonate material. From Rogoz, Sawlowicz, and Wojtal 2012.

Parker and Toots (1970, 931) state that:

...for whatever physical and/or chemical reasons, bone appears to be a very favorable substrate for deposition of a number of minor elements in amounts far greater than present elsewhere in the diagenetic system. Presumably the comparatively larger surface area of the microcrystalline apatite, presence of organic components, and the surface properties of apatite all influence the deposition of minor elements in fossil bone.

Iron, aluminum, manganese, and potassium have all been shown to enter bone from the soil environment, while calcium and magnesium are generally lost by the bone into the ground (Lambert et al. 1985). Yttrium and fluorine are also diagenetic in origin (ignoring the modern standard of fluorinated drinking water) (Parker and Toots 1970). Strontium, in contrast, comes from diet, and is a common and well-researched indicator of the dietary habits of the populations being studied (Parker and Toots 1970; Pollard 2008). Elements can be taken into the bone either through voids and fissures in the bone, or within the apatite matrix itself. Owing to the bone structure and the large surface area of the microcrystalline apatite, there are a large number of exposed ionic charges favoring extraneous cations and anions to become bonded to the crystal surface (Parker and Toots 1980).

Voids resulting from the decomposition of the organic component can also become filled by impurities in the soil, especially carbonate-rich materials. Iron and manganese compounds are found around Haversian canals and osteocytes. These two elements are also responsible for stains on the bone surface (Rogoz, Sawlowicz, and Wojtal 2012).

Bone is an important material in the understanding and interpretation of archaeological sites and assemblages, as it can identify ancient environments, paleodiet, methods of tool making, ancient diseases and causes of death. Bones yield the most information when intact, when they can be measured, and the surface examined for tooth and cut marks, wear, signs of growth or disease, and evidence of cutting and polishing (Koob 1984). The number and type of bones, as well as their size and shape, and any surface features may indicate predation, hunting, reworking, or other important archaeological evidence (Child 1995).

The preservation of bone can be impacted through many complex pathways including cooking, defleshing, and reworking, as well as by both exposure and burial (Hedges 2002). As the environment plays an important role to bone preservation, chemical alternations can be localized within a single bone (Jans et al. 2002).

Chapter 4: Bone consolidation literature review

4.1 Traditional bone consolidating agents and methods

Bones need to be strong enough to be handled and stored without damage, and the often large quantity of bone material found at sites requires a significant amount of consolidant and time for treatment (Koob 1984).

Consolidants used on bone material since the start of the twentieth century include almost every adhesive known to the conservation field at one time (see Appendix 9.1). Shellac, plant resins, gelatin and protein glues, and waxes were common in the earlier part of the century, and were replaced by synthetic polymers as they were developed starting in the 1930s, and subsequently employed in the conservation field. For example, Alvar (polyvinyl acetal) was widely used for fossil bone until the 1960s, when failing industrial demand led to a halt in production (Howie 1984). The problems caused by these consolidants are as varied as the number of consolidant materials used, and are mainly due to: poor penetration, embrittlement, shrinkage resulting in delamination, yellowing over time, and crosslinking resulting in irreversibility.

Currently, consolidants used for bone are most usually polymer-based (Chadefaux et al. 2008) in aqueous or solvent solutions, emulsions, or colloidal dispersions (Johnson 1994). A popular consolidant for damp or waterlogged bone is Acrysol WS-24 and its British equivalent Primal WS-24, an acrylic colloidal dispersion which has close to neutral pH and has shown to be quite stable over time (Johnson 1994). Paraloid B-72, a methyl methacrylate/ethyl acrylate copolymer, is the other consolidant most used by archaeologists and conservators. It cannot be used with damp or wet material, due to its poor performance with water, but for dry material it has shown good working and ageing properties (Koob 1986). While polymer consolidants change significantly the physiochemical behavior and texture of the original material, they do not alter trace element distribution, which is important for any subsequent isotopic analysis. Polymer consolidants are also detectable and identifiable using FTIR and other spectroscopic techniques (Chadefaux et al. 2008).

However, there are still some challenges with today's commonly used polymer consolidants. The high evaporation rate of most solvents can lead to only superficial penetration of the consolidating agent. In addition, many polymer-based consolidants contain high levels of plasticizers and emulsifiers, often proprietary (Koob 1984). In practice, consolidant penetration has been found to be more successful using multiple dilute applications, however this was tested using immersion as the method of consolidation (Koob 1984; Chadefaux et al. 2008), which is often not possible in the field. While immersion may be the best method for ensuring even application and penetration (Koob 1984), deposition onto the surface by brush or poulticing is a more common method of consolidation when the bone is fragile and cannot be removed from the location it was found.

Recent research on alternative consolidating agents leads to the application of new inorganic consolidants being tested on bone and fossil material. Conservare OH100, a low viscosity alkoxysilane, has shown good performance at consolidating previously block-lifted paleontological bones, which were very fragile due to minimal fossilization (Biscula, Elkin, and Davidson 2009). These fossils had been treated in the field with Butvar B-76 (a thermoplastic polyvinyl butyral resin), then lifted and transported to the lab for micro-excavation. Butvar B-76 seems to have consolidated only the surface and as a consequence many of the lifted blocks began to collapse before they could be re-treated. Conservare OH100 on the other hand, was able to compensate for the superficial Butvar B-76 treatment, and successfully strengthen the fossils without fixing the soil around them, allowing for easy mechanical removal.

However, there are some concerns using Conservare OH100 as a consolidant. It requires three months to cure, during which the blocks cannot be worked on. The treatment is also irreversible, although the Conservare OH100 allows future retreatment with polymer-based adhesives. It is also only detectable by a higher silicon signal in SEM-EDS. Further study is needed to fully understand how Conservare OH100 works as a consolidant for bone and fossil, and whether its drawbacks make it less suitable for use at a larger scale in bone conservation.

Chapter 5: Materials and methods

To test the development and evaluation of hydroxyapatite as a consolidating agent for bone and other similar archaeological matrices, experimental laboratory trials were conducted by

applying DAP solutions (at different molar concentrations) and selected organic consolidants on three substrates: bone flour, modern and archaeological bone. The results were evaluated using different structurally-and compositionally-sensitive analytical techniques and methods.

5.1 Materials

5.1.1 Substrates: bone flour, modern and archaeological bone

Bone flour was purchased from MP Biomedicals. This is a finely ground bone meal often used as a dietary supplement for animals. XRD analysis was performed on a sample of the bone flour (See Appendix 9.2), revealing that HAP was the major component, along with a few unidentified peaks, which were assumed to be from collagen or other organic content.

Both modern and archaeological bone samples were procured from Dr. Thomas Wake, director of the Zooarchaeology Lab at the Cotsen Institute of Archaeology at UCLA. The modern bone samples were cut from the femur of a domestic pig (*Sus domesticus*). The archaeological bone samples are of an unidentified animal from a coastal site in the Channel Islands, California, and are approximately 3000 years old.

5.1.2 Consolidants tested

Three different consolidating agents were tested:

1. **Diammonium hydrogen phosphate (DAP)**, used as the precursor for the precipitation of hydroxyapatite, purchased from Fisher Scientific, and prepared at 0.5M, 1.0M and 2.0M concentrations;

2. **Paraloid B-72** (ethyl methacrylate-methyl acrylate copolymer), from Conservation Resources, prepared in a 3% solution w/v in a 1:1 by volume ethanol-acetone solvent mixture;
3. **Acrysol WS-24** (acrylic emulsion of polyacrylic acid mixed with acrylic copolymers or sodium polyacrylate), from Talas, diluted 1:1 v/v with deionized water.

The traditional organic consolidants chosen for testing along with the DAP solutions were selected based on a number of criteria:

- performance in the field of conservation;
- stability and ageing properties;
- known use on bone and bone objects;
- being representative of both aqueous and non-aqueous consolidation methods.

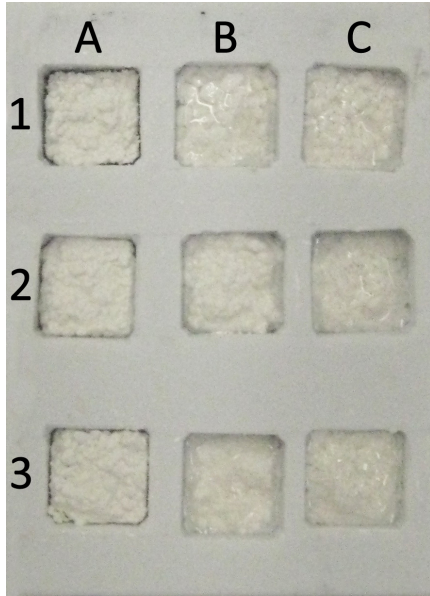
The three consolidants were tested on the bone flour samples and on samples of both modern and archaeological bone. The bone flour tests were used to determine: a) the potential of consolidation by evaluating how well the bone flour grains were kept together after treatment and b) changes in porosity and wettability. Both the modern and archaeological bone samples were evaluated in terms of surface topography and porosity changes.

5.2 Application methodology

5.2.1 Application of consolidants on the bone flour samples

5.2.1.1 Test 1a

To determine the appropriate DAP molar concentration that could provide the best results in terms of consolidation without significant loss of porosity, three different concentrations of DAP solution were tested on the bone flour samples: 0.5M (~6.5%), 1.0M (~13%), and 2.0M (~26%). 0.4ml of each of these three concentrations of solution were applied by dropping from a syringe (at a distance of 1cm from the surface) to 0.5g bone flour compacted in a silicone mold (Figure 5). While the 0.5M solution showed good wetting properties, the 1.0M and 2.0M did not penetrate easily into the bone flour, and the drops of solution remained on the surface. To improve the wettability of the bone flour surface during the testing, drops of ethanol were applied prior to treatment with DAP. The samples were allowed to sit undisturbed for one week before evaluation of the treatment.



	A	B	C
1	0.5M DAP	1.0M DAP	2.0M DAP
2	0.5M DAP	1.0M DAP + 1 drop C ₂ H ₅ OH	2.0M DAP + 1 drop C ₂ H ₅ OH
3	0.5M DAP	1.0M DAP + 2 drops C ₂ H ₅ OH	2.0M DAP + 2 drops C ₂ H ₅ OH

Figure 5. Silicone mold with bone flour samples, after testing. Column A was consolidated with 0.5M DAP, column B with 1.0M DAP, and column C with 2.0M DAP. In addition, 2B and 3B received one drops of ethanol prior to consolidation, while 2C and 3C received two drops of ethanol, to improve the wetting and penetration of the consolidant.

5.2.1.2 Test 1b

The same test was repeated on new set of bone flour samples. After treatment, however, these samples were embedded using a blue-dyed Buehler EpoxiCure® epoxy resin. The resin was first heated to approximately 60°C and Orasol blue dye was added until a strong blue color was achieved. The mixture was stirred continuously for ~10 minutes and allowed to cool to room temperature. EpoxiCure® Epoxy Hardener was added in a ratio of 5:1 wt% resin to hardener. The samples were impregnated under vacuum using a Buehler Cast n' Vac 1000 for ~1 hour,

before being allowed to cure overnight. Once the resin was set, the samples were cut in half using a Buehler Isomet Low Speed Saw.

5.2.1.3 Test 2

A slightly modified test was also performed to compare the performance of DAP against B-72 and Acrysol. The same polymer-based consolidants (3% B-72 in 1:1 acetone:ethanol, and Acrysol WS-24 diluted 1:1 with deionized water) were each tested by applying 0.4ml of each consolidant by dropper to 0.5g of bone flour held in the silicone mold. One drop of ethanol was applied to the bone flour samples prior to the application of the 0.5M and 1.0M DAP solutions. The samples were allowed to sit undisturbed for one week before evaluation of the treatment.

5.2.2 Application of organic consolidants and DAP precursor on modern and archaeological bone samples

The same three consolidants were applied to both the modern pig and archaeological bone samples. Paraloid B-72 and Acrysol WS-24 were applied by dropper to the surface of the bone samples (pre-wetted with ethanol to improve the wetting properties). The DAP solution was then applied by a cotton poultice placed over a barrier layer of Hollytex fabric (nonwoven spun-bonded polyester textile) to prohibit the cotton fibers sticking on the bone. The poultice was then covered with food-grade plastic wrap to slow down the evaporation. The poultice was left on the surface for approximately 2 hours. After the removal of the poultice, the surface of each sample was carefully cleaned using a cosmetic sponge dampened with deionized water, to remove any residues from the sample's surface. The samples were then allowed to sit for two weeks before evaluation.

The results from the trials on the bone flour and modern bone samples were used to determine the best reactant concentrations and application method for testing the archaeological bone samples. Based on the water drop absorption tests and examination using digital microscopy and SEM-EDS imaging and microanalysis on the modern bone samples (see Sections 6.1.1-6.2), 1.0M DAP was chosen as the ideal solution concentration. The 1.0M DAP solution was applied to one side of two archaeological bone samples by poultice and left on the surface for two hours. The poultice was removed and the surface cleared with deionized water to remove residual reactive reagents. After the removal of the poultice, it was observed that it had turned to a dark yellow-brown color. X-ray fluorescence (XRF) spectroscopy and x-ray diffraction (XRD) of the residues in the poultices (see Appendix 9.3) was inconclusive; it is assumed to be residual soil from burial.

5.3 Characterization methods

5.3.1 Digital microscopy (DM)

All treated samples were examined and imaged before and after treatment using a Keyence VHX-1000 digital microscope, utilizing up to 200x magnification, three-dimensional (3D) surface reconstruction, and topographic mapping. The modern and archaeological bone samples were both imaged and mapped before and after treatment, to allow for visual comparison of topographic changes on the samples' surfaces.

5.3.2 Scanning electron microscopy (SEM) and energy dispersive X-ray spectroscopy (EDS)

All samples were examined and imaged using a Nova™ NanoSEM 230 scanning electron microscope at variable pressure (VP) mode before and after treatment. The SEM allowed for

much higher magnification and resolution enabling the study of individual crystals and other surface features at the micron and nano scale. Elemental analysis was performed using a Thermo Scientific NORAN System 7 X-ray Energy Dispersive Spectrometer.

5.3.3 X-ray diffraction (XRD)

XRD analysis was performed using a Rigaku R-Axis Spider X-Ray diffractometer. XRD spectra were recorded at 50 kV/40 mA using a Cu-K α target for 900 seconds. XRD data was processed and matched against reference spectra from the International Center for Diffraction Data (ICDD) files using the JADE v8.2 software from Materials Data Inc. The Rigaku can perform both powder and single crystal structural analysis, which allowed for examination of the bone flour samples both before and after treatment (see Appendix 9.4). XRD analysis was performed to determine changes in crystallinity of the samples, as well as to identify any impurities in the purchased samples.

5.3.4 Water drop absorption

Water drop absorption tests were performed before and after treatment on all samples. In this test (adapted from Teutonico 1988), a drop (~0.05ml) of deionized water is released from a dropper onto the surface of the sample from a distance approximately 1cm from the surface. The time required for the total absorption of the water is determined as (t_n) for the reference (untreated) samples, (t_x) for the treated samples. Evaporation time (t_e) of the drop is measured by releasing a drop of water on a rough glass surface (maintaining the same T and RH conditions). Time is measured using a stopwatch. The water drop absorption (WA) of the treated samples is calculated as a percentage following the formula:

$$WA(\%) = \left[1 - \frac{t_x - t_n}{t_x} \right] \times 100$$

t_x = absorption time into a treated surface

t_n – absorption time into the reference (untreated surface)

For $t_x > 0.05 (t_e)$ the formula becomes:

$$WA(\%) = \left[1 - \frac{t_x - t_n}{t_e - t_n} \cdot \frac{t_e}{t_x} \right] \times 100$$

t_e = evaporation time

Water repellency may be expressed as $WR (\%) = 100 - WA$

For statistical accuracy, the drop absorption test was repeated multiple times and mean and standard deviation values were calculated.

Chapter 6: Results

To evaluate the consolidation potential and to monitor any changes to the properties of the bone matrices, samples were examined for changes in surface and physiochemical characteristics: wettability, water absorption, porosity and surface topography. Structural

properties (adhesion and strength) were not evaluated and will be the subject of further research.

6.1 Surface wettability and water drop absorption

6.1.1 Consolidation effect and water drop absorption on bone flour samples

Varying the DAP molar concentration on the experimental samples (see Test 1a) affected the rate of water absorption by the sample, the depth of infiltration and consequently the consolidation potential. Comparing tests A1-A3 (0.5M DAP) to B1 (1.0M DAP) and C1 (2.0M DAP) applied over the bone flour without any pre-wetting of the surface, there is a noticeable decrease in the water absorption (WA) as the DAP molar concentration is increased (Figure 6A-B). The addition of ethanol prior to consolidation in tests B2 (1.0M DAP + 2 drops C_2H_5OH) and B3 (1.0M DAP + 2 drops C_2H_5OH) show an increase of WA compared to B1. Tests C2 (2.0M DAP + 2 drops C_2H_5OH) and C3 (2.0M DAP + 2 drops C_2H_5OH) on the other hand show significant decrease of WA in relation to C1. This may suggest differential distribution of the consolidant affecting the overall water intake by the sample.

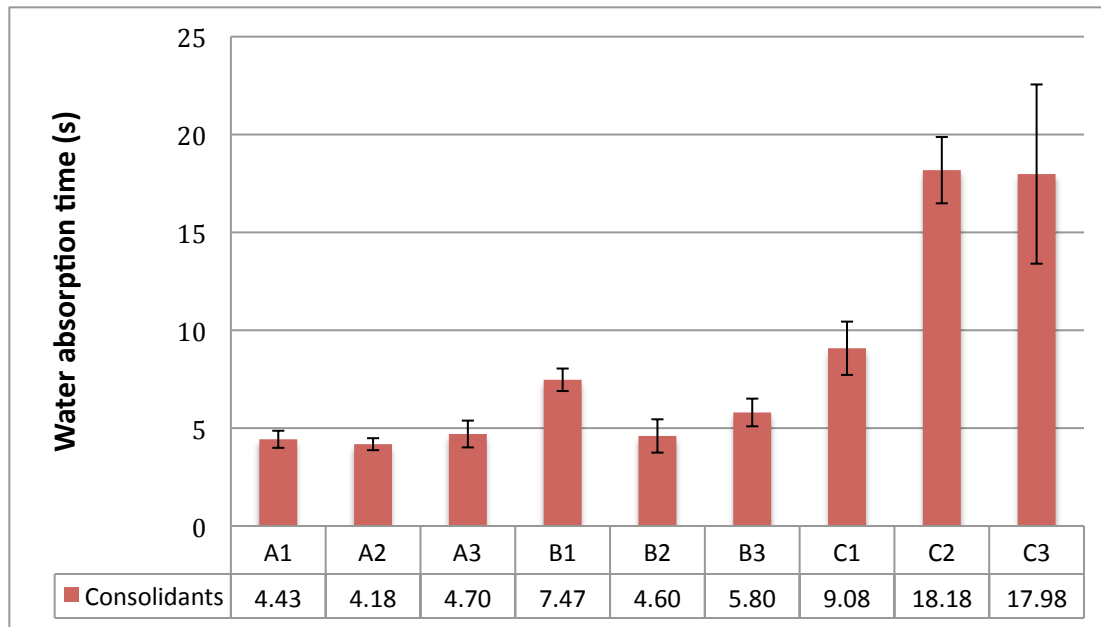


Figure 6A. Results illustrating the water absorption time in seconds of the mean values (N=6 for each) of tests A1-A3, B1-B3, and C1-C3 using 0.5M, 1.0M and 2.0M DAP solutions (see table in Figure 5) on bone flour samples. Reference water absorption time=4s.

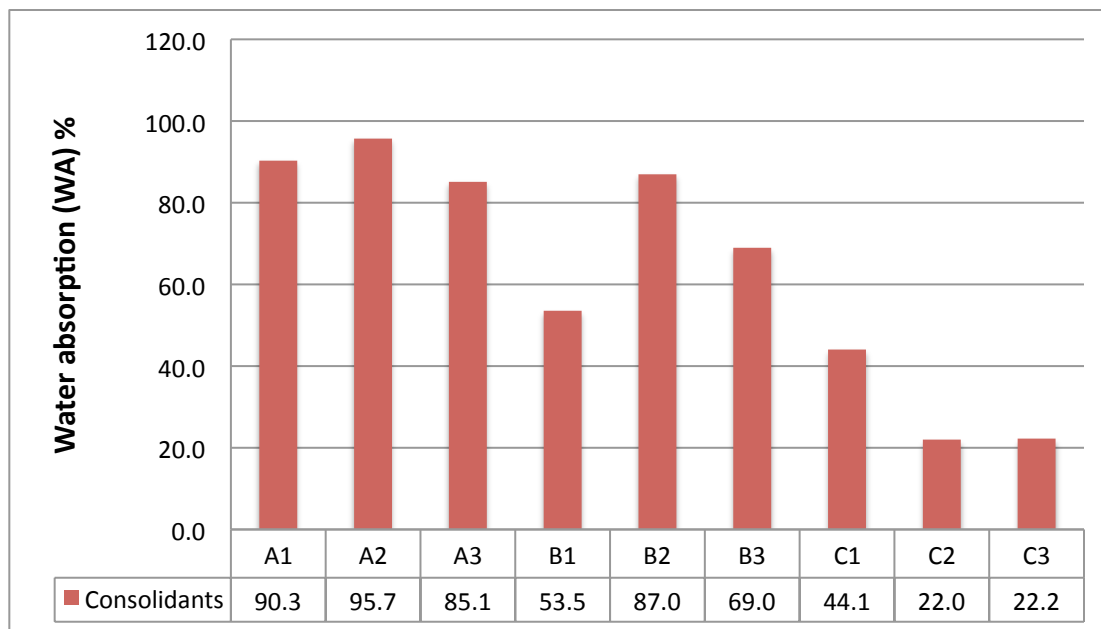


Figure 6B. Results illustrating the water absorption (WA) % – normalized to the absorption of the reference/untreated sample – of the mean values (N=6 for each) of tests A1-A3, B1-B3, and C1-C3 using 0.5M, 1.0M and 2.0M DAP solutions (see table in Figure 5) performed on bone flour samples. Reference water absorption time=4s.

Porosity also seems to be inversely affected by the concentration of the DAP solution. However, further investigations are required to establish whether the consolidant has truly affected the bulk porosity or if it has only created a more compact layer on the surface. The rate and degree of impregnation of treated bone flour samples under vacuum with colored epoxy (Test 1b, Figure 7) provides a visual representation of the effect of the different concentrations of DAP on the assumed porosity of the bone flour samples. Keeping the time of vacuum impregnation constant (~45 minutes), samples treated with 0.5M DAP solution (Figure 7A-B) showed almost complete and even distribution of the blue-colored epoxy resin in the bulk of the sample. Samples treated with 1.0M DAP (Figure 7C-D) showed a gradient with the outermost ~0.5 mm fully impregnated (dark blue), the next ~0.5 mm slightly impregnated (light blue), and the core unimpregnated (white color of the bone flour). The samples treated with 2.0M DAP (Figure 7E-F) show no evident impregnation by the epoxy, except where the sample has cracked. This indicates either a reduction in porosity by the consolidating treatment, or water repellency of the surface caused by hydrophobicity.

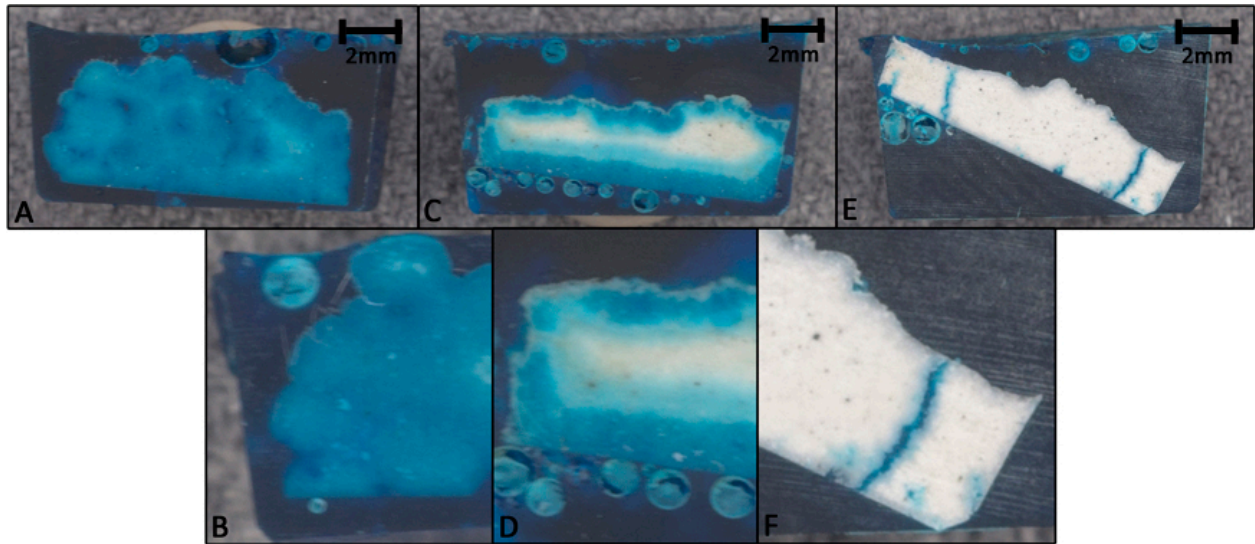


Figure 7. Photomicrographs of bone flour samples impregnated with blue colored resin. A-B: 0.5M, C-D: 1.0M, E-F: 2.0M treated samples. Photomicrographs B, D, and F are higher magnifications of photomicrographs A, C, and E.

Following these results, 2.0M DAP concentration was eliminated from further testing, as it greatly decreased water absorption of the samples after treatment.

The results of Test 2 could not be adequately measured. The Paraloid B-72 treated sample formed a film on the surface with very shallow consolidation. Attempts to remove the sample from the silicone mold after testing resulted in the upper consolidated surface shattering, revealing powdery/unconsolidated bone flour underneath (Figure 8). The Acrysol WS-24 treated sample could be removed from the mold easily as a solid block, but drop absorption tests showed no noticeable absorption, indicating water repellency.

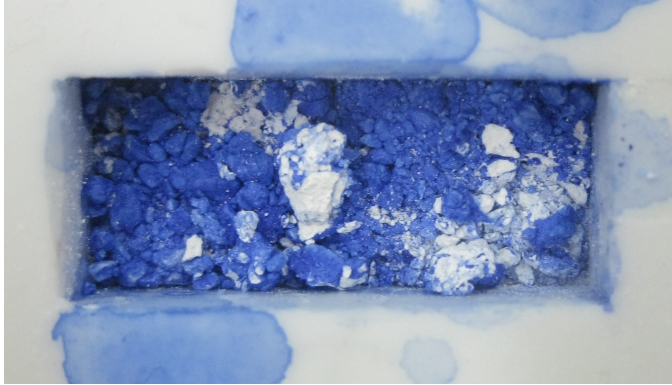


Figure 8. Bone flour sample treated with 3% B-72, which broke upon trying to remove it from its silicone mold. Pigmented B-72 was used in an attempt to better visualize the consolidant penetration via cross-sectioning, but the lack of consolidation to the sample made this impossible.

6.1.2 Water drop absorption of modern bone samples

Water drop absorption tests on the modern bone specimens indicated that both Paraloid B-72 and Acrysol WS-24-consolidated samples formed an impermeable layer on the surface. The time for total water drop absorption was equal to the evaporation time from a non-absorbing surface showing characteristics of water repellency. The 0.5M and 1.0M DAP treated samples show a change in the wettability of the surface resulting in reduced water absorption times, especially for the 1.0M DAP test (Figure 9A and B). It is not clear what causes this change in wettability and further analysis will be conducted.

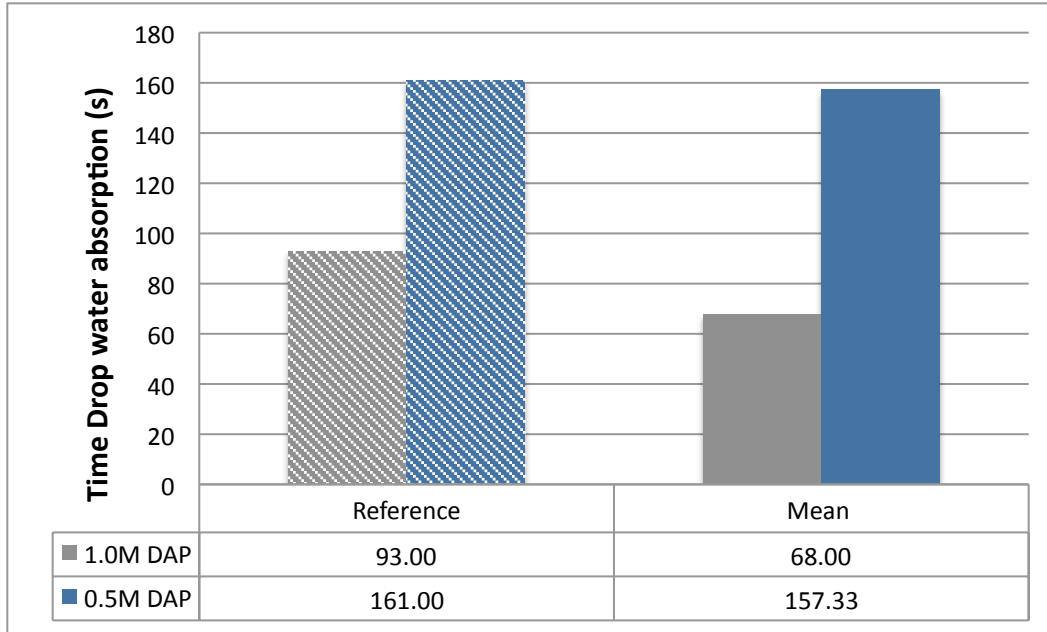


Figure 9A. Results of water absorption tests on modern bone samples treated with 0.5 and 1.0 M DAP solutions respectively before (reference sample) and after treatment (mean N=3). As it can be seen from the graph there is a change in wettability of the surface resulting in reduced absorption times of the treated areas, especially for the 1.0M DAP treated area.

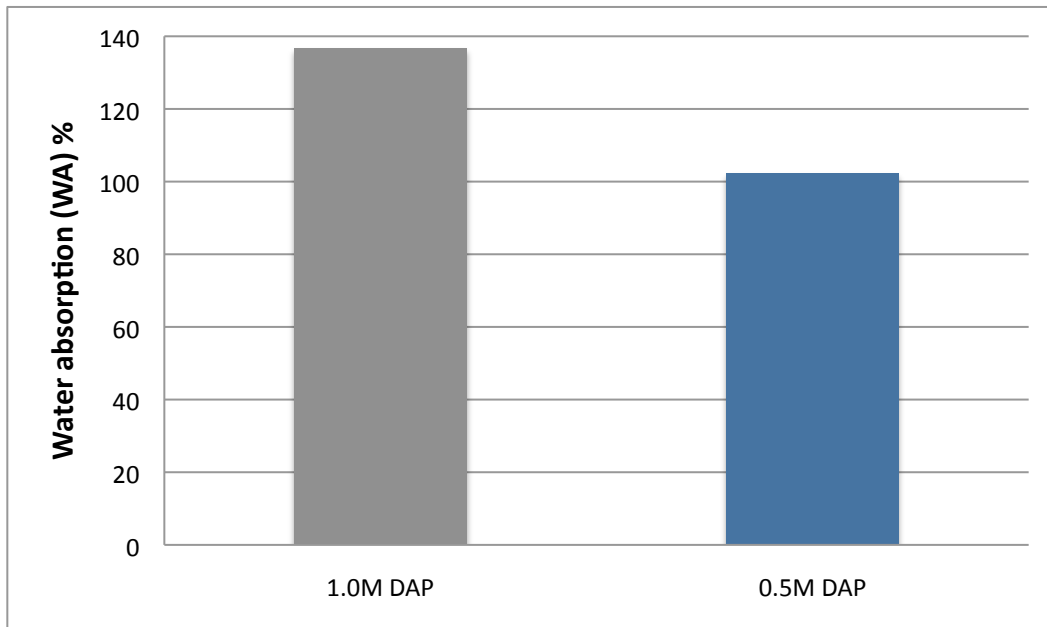


Figure 9B. Results illustrating the water absorption (WA) % – normalized to the absorption of the reference/untreated sample – of the mean values (N=3 for each) of tests using 1.0 and 0.5 M DAP solutions. Considering that the absorption of the reference untreated surface is set equal to 100% the high increase especially for 1.0M indicates a change of the surface wettability and an unexpected anomaly in the measurements.

6.1.3 Water drop absorption of archaeological bone samples

Water drop absorption on the archaeological samples before and after treatment showed retardation of water absorption after consolidation, with the exception of sample Arch 1, side B where the water absorption time is shorter than the reference sample, resulting in WA% above 100% (Figure 11A and B). All other surfaces treated showed a reduction in overall WA%. The reduction in absorption time for Arch 1 side B is only very slightly greater than the standard deviation, and more analysis is needed to understand the anomaly.

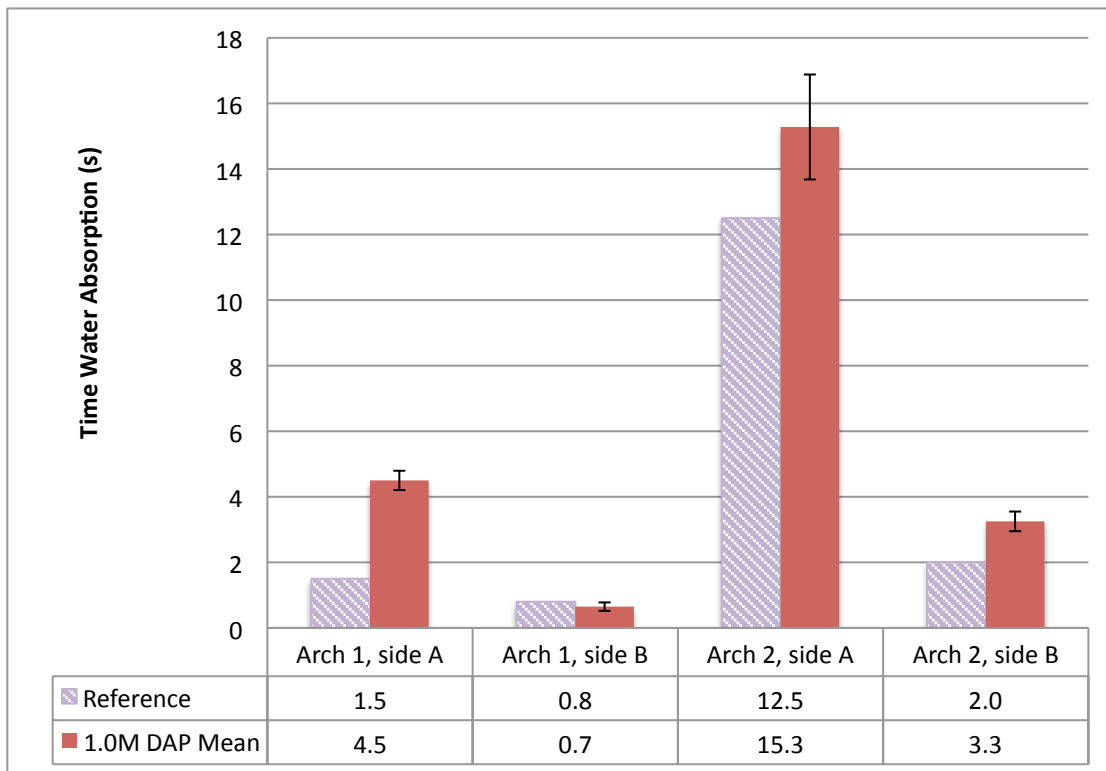


Figure 10A. Results of water absorption tests on archaeological bone samples (Arch 1 and Arch 2) treated with 1.0 M DAP solution before (reference sample) and after treatment on both sides of each sample: side A (surface in contact with the poultice) and side B (back surface away from the poultice). As it can be seen from the graph there is a slight change in wettability of the surface in sample Arch 1, side B resulting in reduced absorption time.

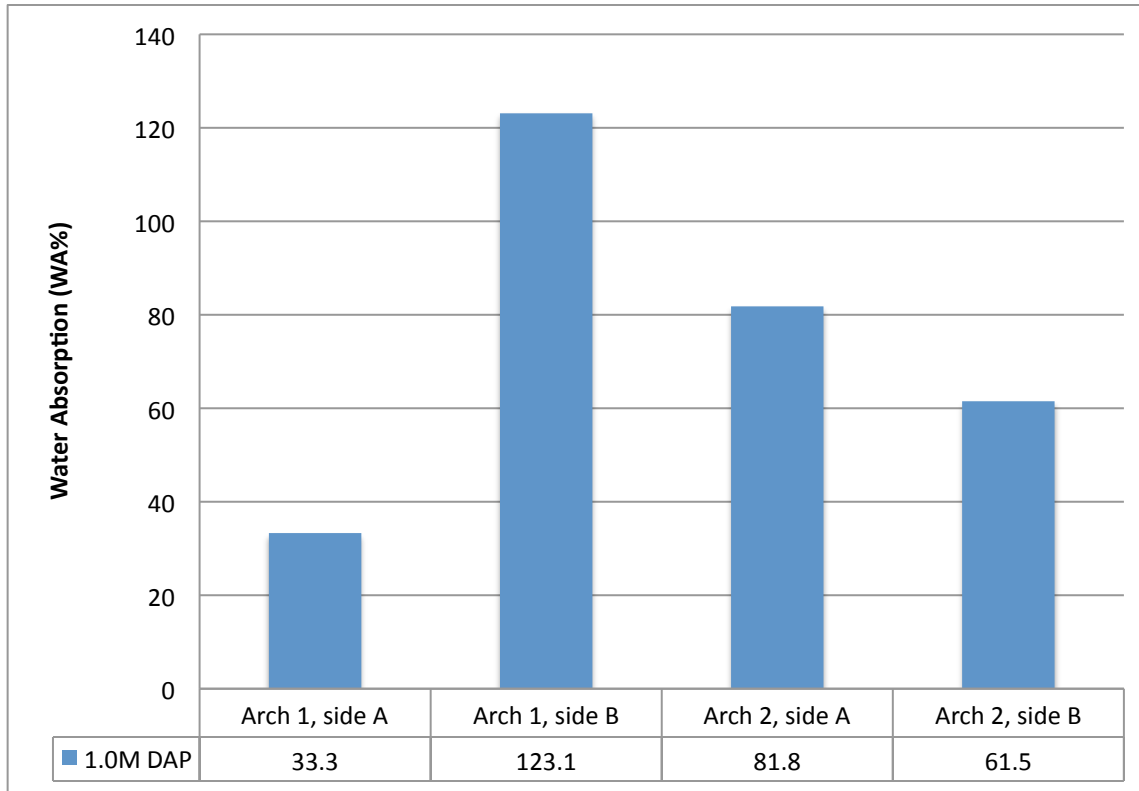


Figure 10B. Mean values (N=4) of water absorption (WA%) for the archaeological samples treated with 1.0M DAP measured on two sides of the bone: side A (surface in contact with the poultice) and side B (back surface away from the poultice).

6.2 Digital (DM) and scanning electron microscopy (SEM)

6.2.1 Modern bones samples

Surface topography and porosity are clearly affected by the polymer-based treatments, as both DM and SEM imaging of the treated modern bones reveals smooth, glossy surfaces with filled pores, in contrast to the reference (untreated) samples (Figure 11-Figure 12). Figure 11 displays DM (A-B) and SEM (C-D) micrographs of the surface topography of a sample treated with Acrysol and Figure 12 illustrates the DM (A-B) and SEM (C-D) micrographs of a sample treated with Paraloid B-72.

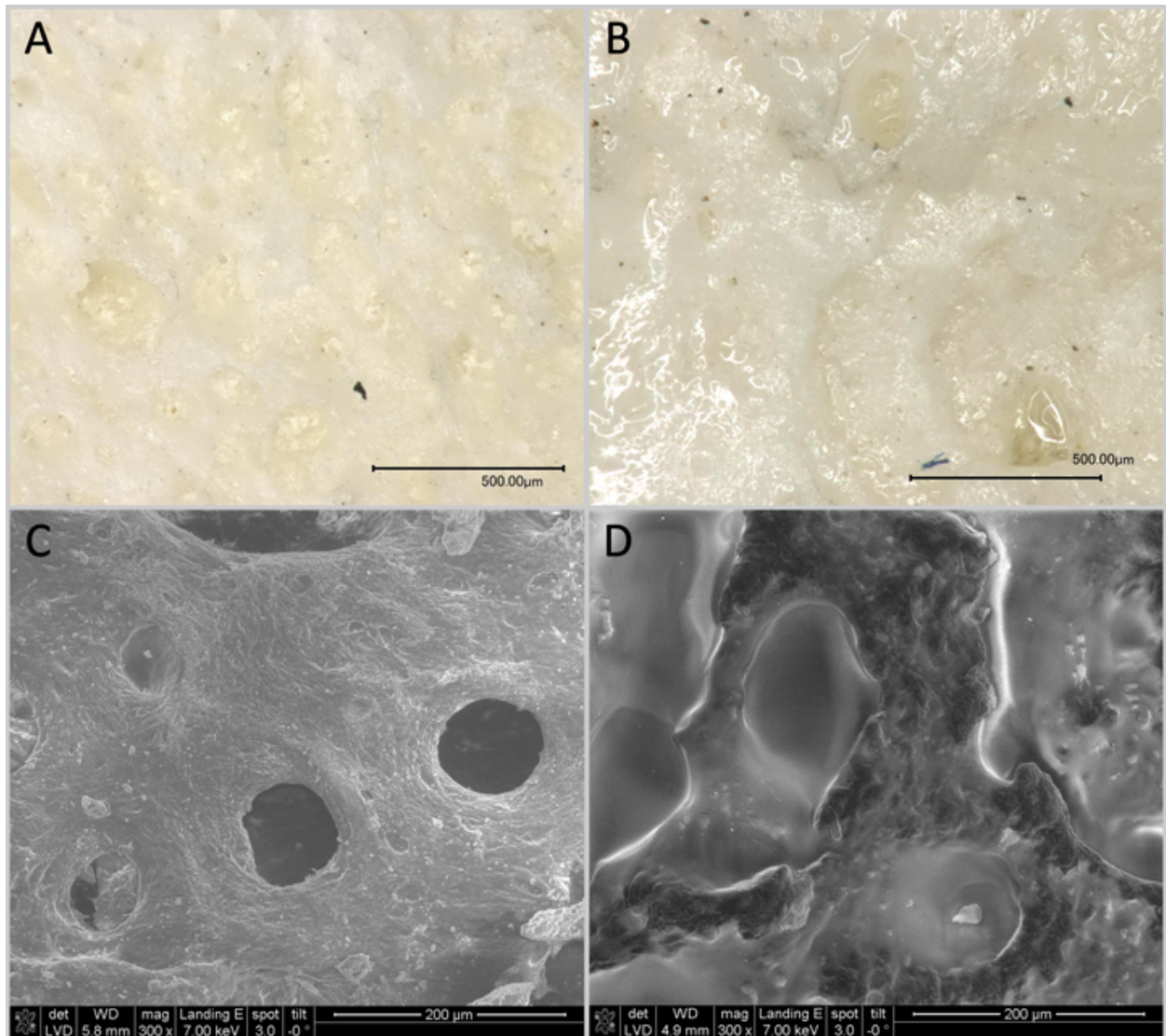


Figure 11. DM and SEM photomicrographs of the reference sample (A and C) and sample treated with Acrysol WS-24, with B and D clearly showing the difference in surface porosity and topography after treatment. After treatment the texture of the surface shows a glossy finish (B) and the pores (C) are clearly filled with the consolidant (D).

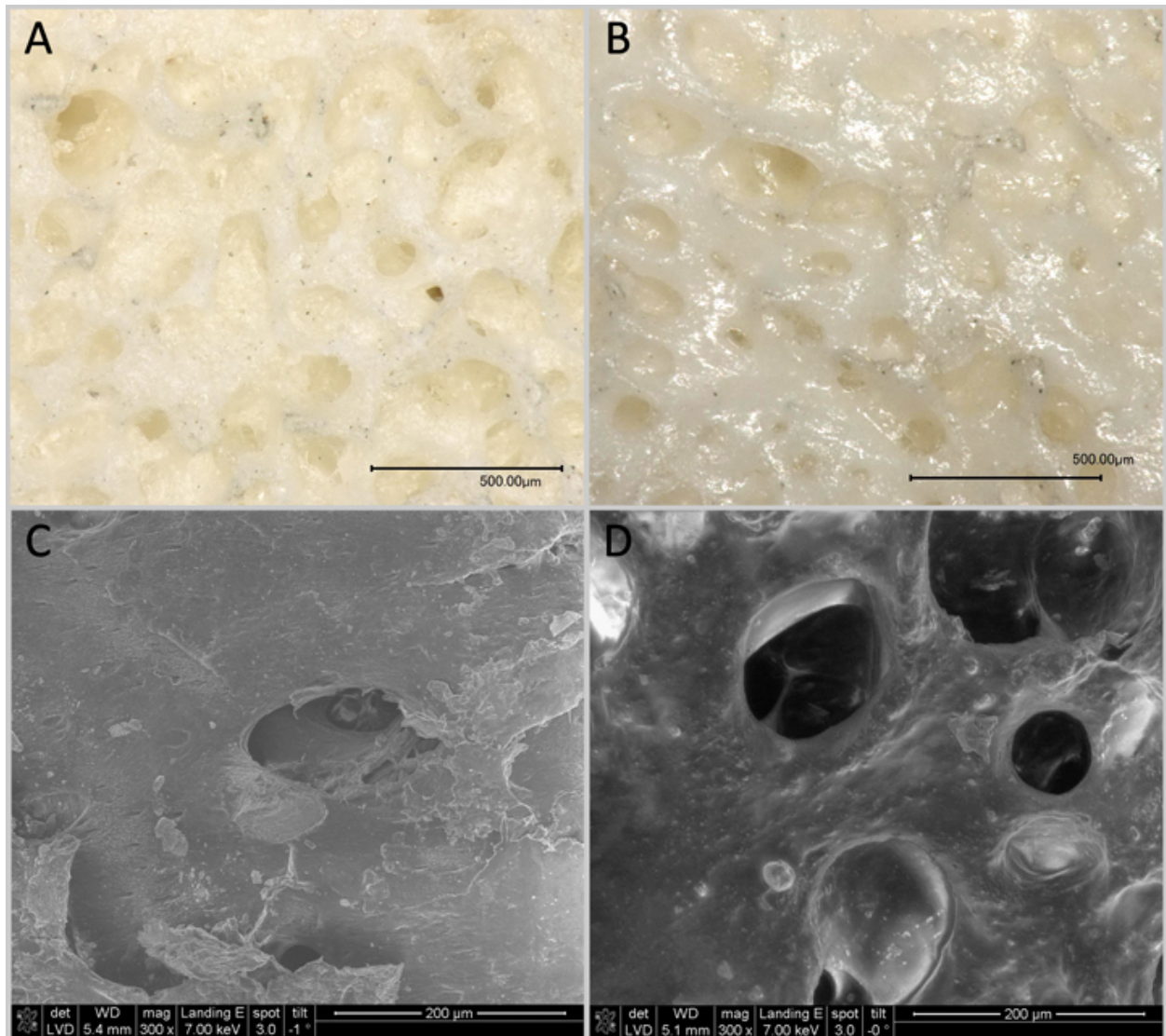


Figure 12. DM and SEM photomicrographs of the reference sample (A and C) and treated with Paraloid B-72, with B and D clearly showing noticeable differences in surface porosity and topography after treatment. After treatment, the texture of the surface shows a glossy finish (B) and the pores (C) are clearly filled with the consolidant (D).

The DAP treated (0.5M and 1M) modern bone samples showed no significant change in the surface topography and texture. Also, the pores of the bone remained open without any visible clogging. The treatment however, revealed newly formed crystals on the bone surfaces and within pores (Figure 13). The crystals are generally orthorhombic in habit, though vary in size, averaging around 30-80 mm at the longest dimension (see Appendix 9.5.1).

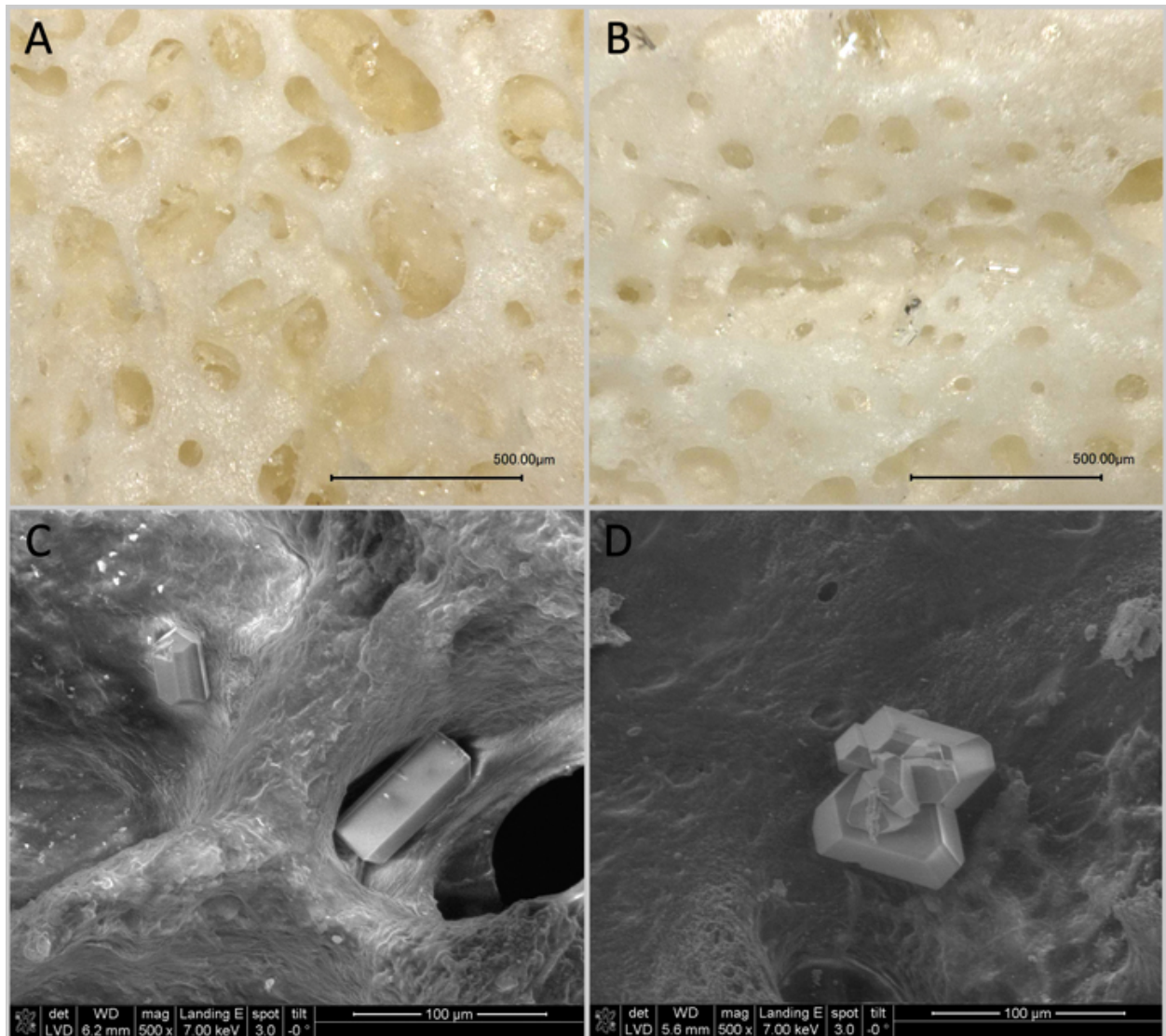


Figure 13. DM (A-B) and SEM (C-D) micrographs of crystals formed on the surface of both the 1.0M (A and C) and 0.5M (B and D) treated modern bone samples.

EDS analysis showed the emission of characteristic X-rays of magnesium (Mg), phosphorous (P), and nitrogen (N) suggesting the formation of magnesium ammonium phosphate (struvite) salt

($\text{NH}_4\text{MgPO}_4 \cdot 6\text{H}_2\text{O}$) (Figure 14). All crystals with similar morphology and habit in the modern bones analyzed showed the same elemental composition (see Appendix 9.5).

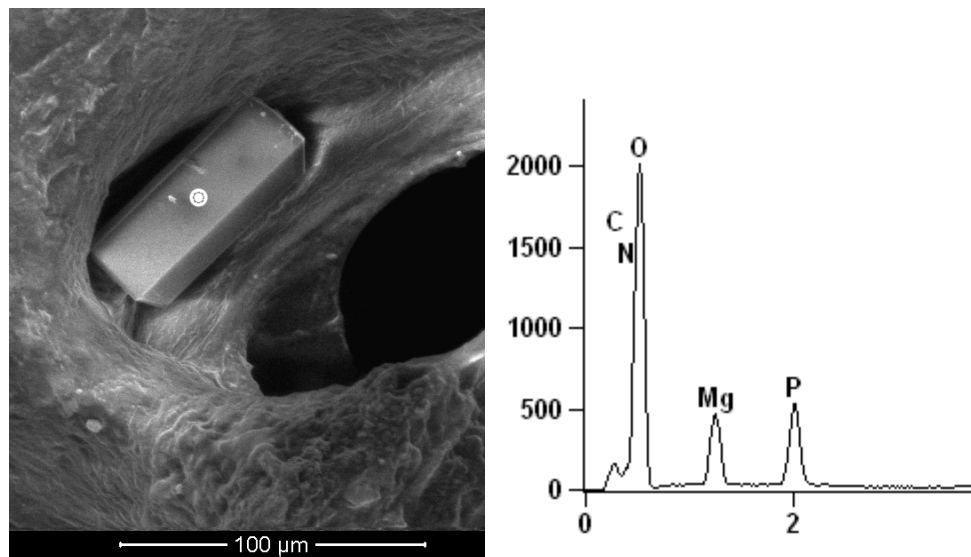


Figure 14. SEM micrograph (left) and EDS spectrum of the orthorhombic crystal found on the modern bone treated with 1.0M DAP. The white circle on the SEM image shows the location of the EDS spot measurement.

6.3 Archaeological bone samples

Similar to the modern bone samples, the archaeological samples did not show any obvious changes in the surface topography and porosity. SEM imaging revealed precipitated crystals of struvite on the surface of all the treated samples, but of significantly smaller sizes than those seen on the modern bone samples (Figure 15). There also seemed to be fewer per surface area (mm^2) in the archaeological samples.

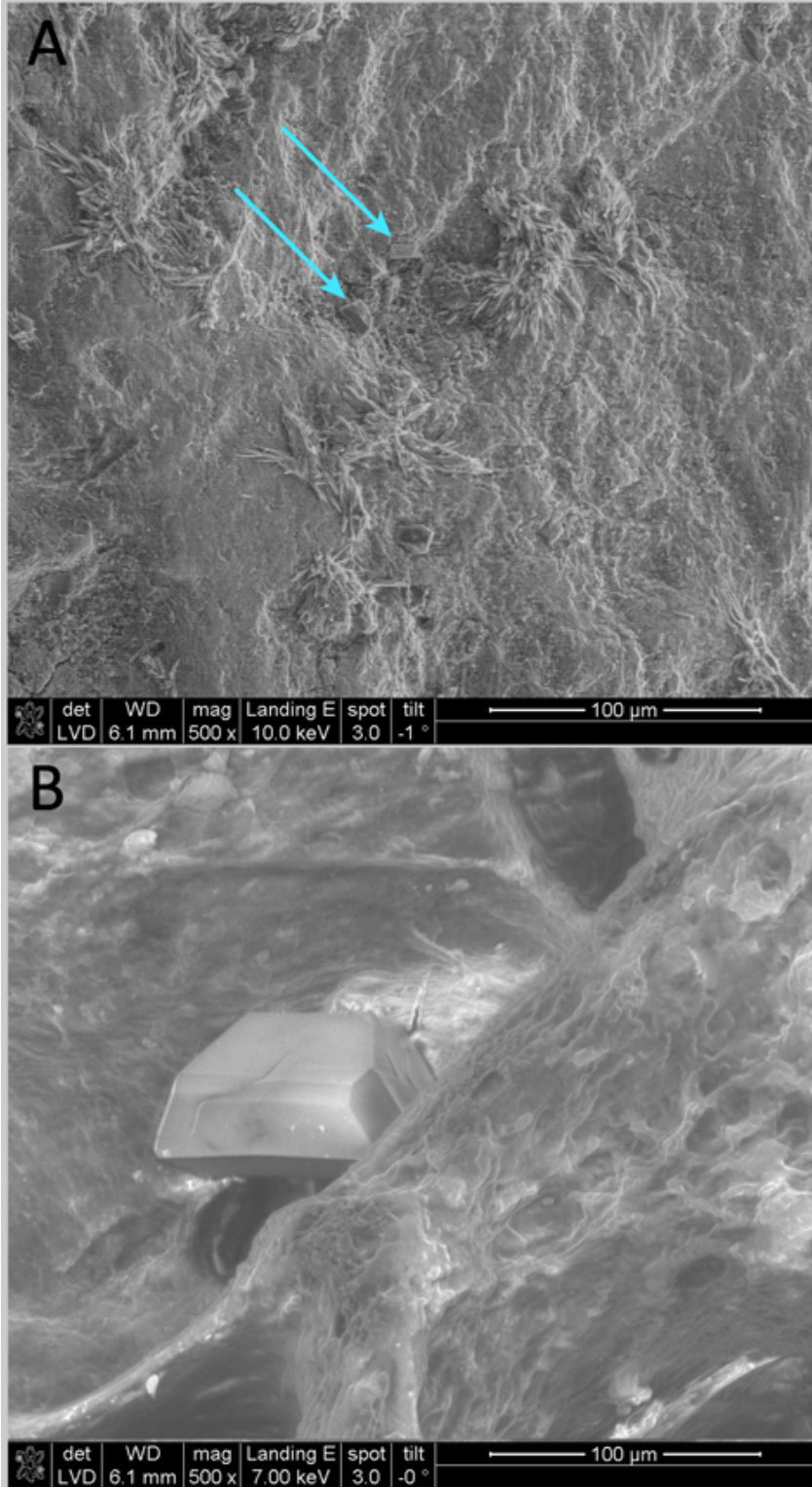


Figure 15. SEM micrographs of the surface of an archaeological bone sample (A) and modern bone (B) both treated with 1.0M DAP. Surface crystals found on the modern bones are many times larger than those found on the archaeological samples (indicated by the arrows).

The archaeological samples also formed long, needle-like crystals on their surface (Figure 16) after treatment. EDS showed these crystals to be a form of calcium-deficient calcium phosphate. They were often associated with magnesium phosphate crystals.

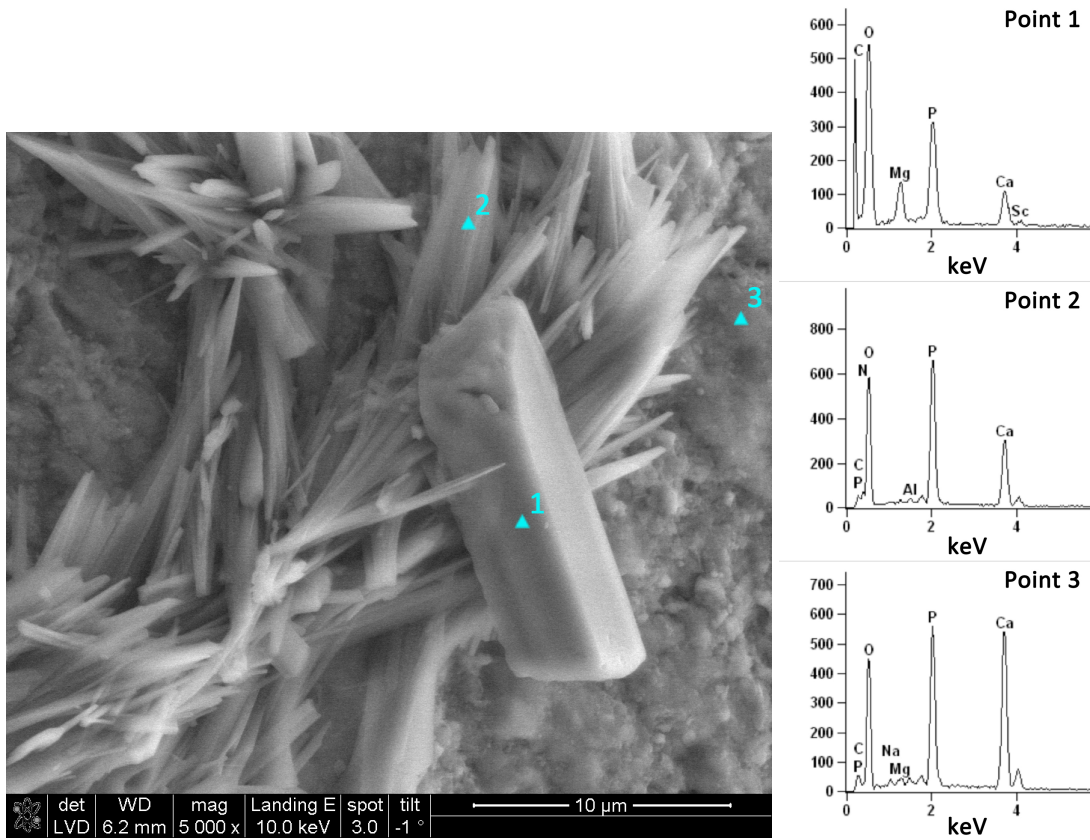


Figure 16. SEM-EDS micrograph and EDS spectra revealing the elemental composition of the magnesium phosphate (1) orthorhombic-like crystal, needle-like calcium-deficient calcium phosphate crystals (2), and original bone surface (3).

Chapter 7: Discussion

7.1 Surface wettability and sorptivity

Overall, the water drop absorption tests indicated that DAP solutions (0.5M and 1.0M) showed greater promise as consolidating agents for bone than higher DAP concentrations or other polymer-based consolidants.

Assuming that the surfaces treated with DAP are non-hydrophobic, water drop absorption tests indicated that DAP solutions of 0.5M and 1.0M would moderately reduce the intake of water absorption with no risk of water repellency. The 2.0M DAP solution proved to be an inappropriate consolidating agent, as it more greatly reduced the water absorption and surface porosity. Previous studies of the effects of polymer-based consolidants, specifically on archaeological antler (Chadefaux et al. 2008), revealed that the crystallinity was greatly reduced in the treated samples, but that porosity was unchanged. This contrasts the findings here, where the polymer-based consolidants greatly reduced both the porosity and wettability of the bone, showing evidence of water repellency.

In the case of the modern bone samples, the 0.5M DAP solution did not significantly affect the surface wettability, and results of the water drop absorptions tests were comparable to those of the untreated samples. However, treatments using 1.0M DAP showed changes in surface wettability. This atypical behavior requires further investigation. The polymer-based consolidants, however, reduced the surface wettability to values close to water repellency. This may suggest that traditional polymer consolidants, even at dilute concentrations below 3wt%, can significantly increase the hydrophobicity of bone altering its physiochemical behavior.

The DAP-treated archaeological bone samples showed inconsistencies in the WA% ranging from 33-82% for Arch 1, side A and Arch 2, side A and 61-123% for Arch 1, side B and Arch 2, side B respectively. While all surfaces treated with 1.0M DAP showed a noticeable decrease of WA% from the reference sample (with the exception of Arch 1, side B) there is a large deviation among the values that needs further study. The results from sample Arch 1, side B show an atypical and unexpected increase in surface wettability.

7.2 Surface topography and porosity

There is a very noticeable change of the surface topography on all samples treated with Acrysol WS-24 and Paraloid B72. All samples show the presence of a coating covering the surface causing a significant modification to the original topography and texture. Moreover, large pores have been filled with the polymer, which further prohibits water movement. The DAP treatments selected for this study (of 0.5M and 1.0M) on the other hand, showed no obvious surface modifications and the pores remained unblocked.

7.3 Reaction chemistries

7.3.1 Magnesium ammonium phosphate (struvite) formation

The formation of magnesium ammonium phosphate (struvite) crystals in the treated modern and archaeological bone samples was not surprising given that Mg is a common element in bone. It is known that amorphous calcium phosphate will react to form crystalline calcium phosphate, when in the presence of water and excess phosphate anions (Eanes, Termine, and Posner 1967). The relatively high amount of amorphous calcium phosphate within the bone structure should have been an easily utilized source for the DAP solution to use to form

crystalline HAP. However, it seems differences in solubility between magnesium phosphates and calcium phosphates were a stronger driving force than the reaction of the amorphous calcium phosphate to a more crystalline form.

There are different studies on the solubility constants for calcium and magnesium phosphates (Moreno, Gregory, and Brown 1968; Hanhoun et al. 2011). The complexity of the apatite structure in general, and its penchant for substitutions, vacancies and impurities lead to inconsistent results on a specific apatite's solubility. The K_{sp} of HAP specifically has been very hard to definitively identify, due in part to the amorphous form, which complicates the liquid-solid equilibrium (Moreno, Gregory, and Brown 1968; Hanhoun et al. 2011; Dorozhkin 2009). Moreno et. al. were confident in stating that the order of magnitude for the K_{sp} of HAP was 10^{58} , however more recent studies by Dorozhkin identify the K_{sp} of HAP as 10^{-117} .

The solubility of magnesium phosphates also vary, but can be similarly limited to an order of magnitude. Hanhoun et al. show that the K_{sp} of struvite averages around 10^{-14} (2011). This is vastly larger than the identified range for the K_{sp} of HAP, and may explain the reason why magnesium phosphate was preferentially formed. The magnesium cations, initially held on the surface of the HAP crystals, would freely associate with the phosphate in the DAP solution, and as the bone sample dried, the precipitate formed would be a magnesium ammonium phosphate compound. The greater insolubility of HAP would preclude the calcium content already within the bone from coming into solution and being able to react with the phosphate anions in the same way.

In the experiment studying formation of non-biological magnesium phosphate under laboratory conditions, the solid was precipitated out immediately upon mixing the reactants, but the resulting product was found by XRD to be amorphous. Eanes and Posner (1968) found that in the presence of ammonium cations, amorphous magnesium phosphate will take the form of $\text{MgNH}_4\text{PO}_4 \cdot X \cdot \text{H}_2\text{O}$. The amorphous magnesium phosphate was also found to be more stable than amorphous calcium phosphate. The reaction occurring here may be an initial formation of the amorphous magnesium phosphate, followed by the transformation to a crystalline form, such as struvite. The kinetics of this transformation has not been investigated in the scope of this study.

The variation in crystal size between the modern and archaeological samples is also an interesting result. The amorphous forms of calcium phosphate have been shown to be up to an order of magnitude larger than the crystalline forms (Eanes, Termine, and Posner 1967). If bone HAP becomes more crystalline over time (Eanes, Termine, and Posner 1967; Blumenthal and Posner 1973; Price 1989), then the older bones would have in general a smaller amount of amorphous calcium phosphate to react with the DAP, perhaps resulting in the much smaller crystals.

Bone and teeth have a maximum magnesium content of around 2%, or a ratio of twelve calcium atoms to every one magnesium atom (ivory has approximately twice the amount of magnesium) (Freund et al. 2002). Magnesium can be lost from the bone matrix post-burial, but it is also easily reintroduced through the pores (Parker and Toots 1980). While magnesium cannot substitute for calcium directly in the HAP structure (Freund et al. 2002), it remains

present on the outer surface of the HAP crystals, free to react with the applied DAP precursor and potentially form various magnesium phosphate compounds (Eanes and Posner 1970). The significantly larger size of the magnesium phosphate crystals in the modern bone samples compared to the archaeological samples, may be due to a loss of magnesium content in the archaeological samples through diagenetic processes.

7.3.2 Amorphous calcium phosphate

The possible formation of amorphous calcium phosphate in the consolidated bone flour samples indicates that a more complex set of reactions may be taking place than those outlined in earlier conservation publications (Matteini 2010; Sassoni, Naidu, and Scherer 2011; Yang et al. 2011). It seems that the magnesium content in bone, low as it may be, is affecting the formation of crystalline HAP. The presence of magnesium has been shown in multiple earlier studies to affect both the crystallinity and rate of formation of HAP crystals in solution. In the presence of crystalline HAP, amorphous calcium phosphates should autocatalyze to form the crystalline structure (Eanes and Posner 1968; Tomazic, Tomson, and Nancollas 1975). However, the presence of magnesium will stabilize the amorphous calcium phosphate, even when in the presence of fully crystalline HAP (Eanes and Posner 1968; Alkhraisat et al. 2013).

Some of these studies also state that magnesium is excluded from the final calcium phosphate precipitation (Tomazic, Tomson, and Nancollas 1975). This means that while the presence of magnesium cations limits the crystallization of the HAP, it does not react with it in any way, instead forming its own equilibrium: $\text{Mg}^{2+} + \text{HPO}_4^{2-} \rightleftharpoons \text{MgHPO}_4$. While EDS analysis of the modern and archeological bones in this study has attributed crystals formed on the surface

to magnesium ammonium phosphate precipitates, the XRD spectra of the treated bone flour samples do not show any magnesium ammonium phosphate presence (if any, it is below the limit of detection), nor any apparent decrease in crystallinity (see Appendix 9.3).

All bone has a measureable magnesium content in an easily accessible form (present outside the HAP crystal structure) for the reaction to occur, and this may slow or effectively prevent the formation of crystalline HAP from the applied DAP solution. This, however, does not necessarily mean that consolidation will not occur, which has been proven by the bone flour tests. SEM imaging of the bone flour samples after treatment revealed an oddly smooth surface (Figure 17), which may indicate the formation of amorphous calcium phosphate, as well as clusters of HAP (see also Appendix 9.6).

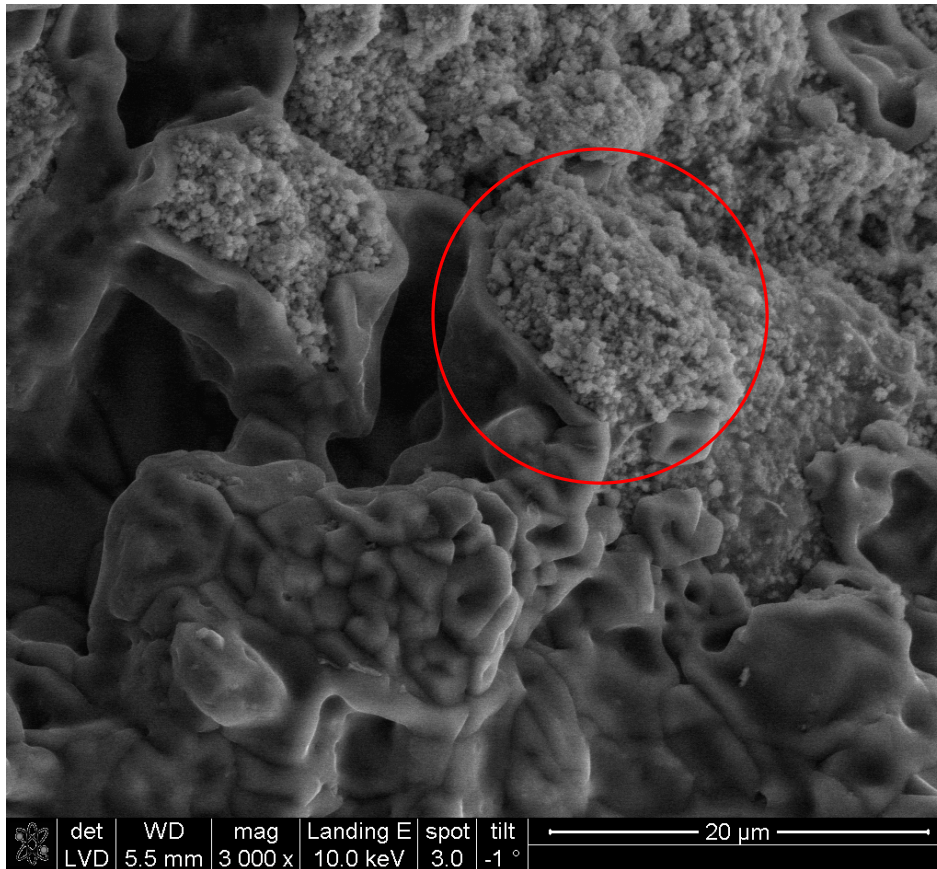


Figure 17. SEM image of 2.0M treated bone flour sample. The area within the red circle resembles hexagonal plate-like crystals of HAP, but this could not be confirmed by other analytical methods.

7.3.3 Calcium-deficient phosphate phases

The molar ratio of Ca:P in ideally stoichiometric HAP should be 1.67, though measured ratios can vary from around 1.4 to 1.7, depending on the source material and method of analysis (Eanes and Posner 1970; Bailey et al. 2009). Biologically derived HAP is calcium deficient, often with additional phosphate anions on the crystal surface, and many other random defects and substitutions. Carbonate can make up as much as 5% of the total bone mineral, although it too

exists mostly on the surface, with only 5-10% being found within the apatite structure (Eanes and Posner 1970).

EDS results (see Appendix 9.7) of the modern bone sample substrates show an average (N=10) ratio of ~ 1.61 , which is quite close to the ideal HAP value. The magnesium values for all the EDS readings averaged 0.24%, much lower than the 2% value listed above. All of the substrate readings also showed a significant carbon and oxygen content, implying the presence of a large amount of carbonate.

EDS measurements of Ca and P in the archaeological sample substrate (see Appendix 9.8) were much lower in carbonate content, with a Ca:P average (N=14) of ~ 1.78 . This is likely due to the increase in HAP crystallinity over time (Hedges 2002), or to a diagenetic loss of carbonate in substituted HAP crystals. Bone can consist of as much as 4-8 wt% carbonate while *in vivo*, which decreases crystallinity and increases solubility (Lee et al. 2007). Carbonate-substituted HAP may then be preferentially dissolved and lost through diagenesis, leaving the bone with a higher Ca:P ratio.

However, the needlelike crystals that formed on the surface of the archaeological bone samples all show low Ca:P values, averaging ~ 0.83 . No magnesium was detected in any of the EDS readings of the needlelike crystals, so it is presumed not to be substituting for the calcium. Instead, it appears that these crystals are a separate development from the magnesium phosphate crystals, though possibly related because they are often found together (Figure 18).

The crystals resemble those of brushite ($\text{CaHPO}_4 \cdot 2\text{H}_2\text{O}$) (cf. Figure 13 in Grases, Costa-Bauzá, and García-Ferragut 1998, 185), which has an ideal Ca:P ratio of 1. The presence of magnesium in the bone matrix may prevent the conversion of brushite to HAP, as the magnesium cations, freed while the aqueous phosphate solution was applied, bind to nucleating sites (Alkhraisat et al. 2013). This magnesium may then react with the phosphate anions, forming magnesium phosphate crystals in association with the brushite.

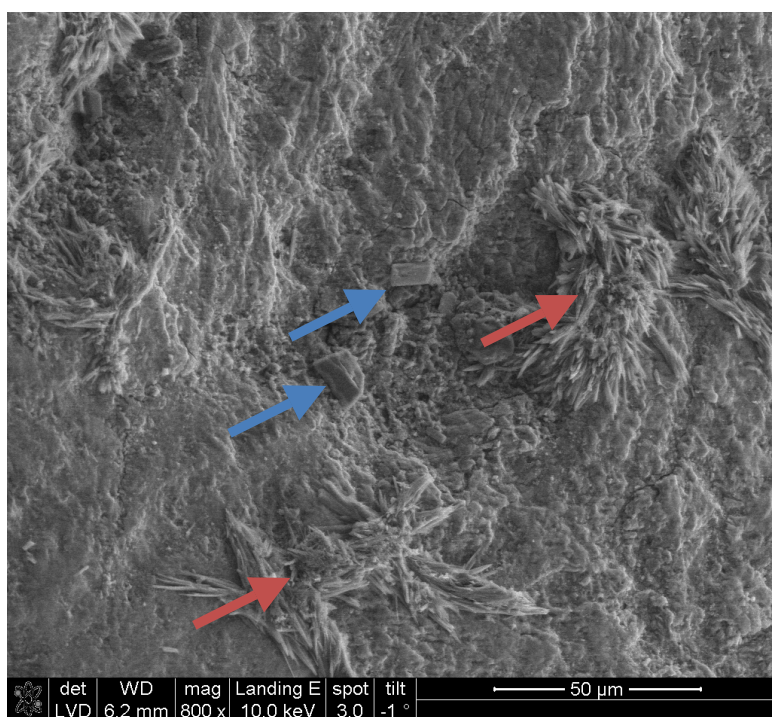


Figure 18. SEM photomicrograph of archaeological bone sample after treatment, showing both magnesium phosphate (blue arrows) and calcium-deficient calcium phosphate (red arrows) formations on the sample's surface.

It is currently unknown why the needlelike calcium-deficient crystals were found only on the archaeological samples. The current assumption is that the increased crystallinity, and/or the

lack of carbonate anions, is responsible for their formation. Further research is needed to better understand their presence.

Chapter 8: Conclusions

The rationale for this research was to address issues in bone consolidation posed by current practices. Organic polymers shrink as they age, can pull or delaminate layers of the surface away, and coatings on the surface may obscure important surface details. Many will also discolor or create a sheen on the bone's surface. High viscosity consolidants also often have poor penetration into the bone, developing highly hydrophobic surfaces. It is also possible that many of these consolidants may affect or prohibit other scientific studies. Isotope analysis, trace element analysis, radiocarbon dating, DNA retrieval, and other investigations may be hindered or blocked by the addition of these consolidants (Johnson 1994).

The use of DAP solutions, already proven as a successful consolidating mechanism for other calcareous materials, has great potential as an inorganic, biomimetic consolidant for friable bone. When compared to traditional polymer consolidants, DAP will consolidate powdery material without introducing incompatible polymeric compounds, and it will not adversely affect the surface appearance or topography, porosity, or significantly alter the wettability of bone.

The results from this study indicate that DAP at concentrations between 0.5 and 1.0M could strengthen weathered bone. The overall performance of DAP treatments was superior from the other materials tested. However, the effects of the increase in surface wettability

observed on the modern and archaeological bone and the formation of struvite and brushite crystals requires further investigations.

8.1 Further Research

8.1.1 Future experimental and theoretical testing

Important basic and applied research still needs to be conducted to better understand the effects of consolidation. This includes:

- Mechanical testing to better understand the strength of bone after application of the various consolidants;
- Artificial accelerated ageing to monitor the behavior of materials (stability, durability) in the long term;
- Basic research on the kinetics of the reaction chemistries and phase transformations using DAP and its effect on surface wettability;
- Introduce desalination treatment prior to consolidation to remove soluble salts and their potential interactions with DAP chemistry;
- Examine and evaluate the potential harmfulness of magnesium phosphate salts (if their formation cannot be avoided) in the long-term preservation of the bones.

8.1.2 Use on teeth and ivory

The issue of the formation of magnesium phosphates may be more pronounced in ivory, particularly elephant ivory, which has a markedly higher magnesium content than bone (Freund et al. 2002). Crystals which spontaneously form on the surface of both natural and worked ivory have been shown to consist of the magnesium phosphates newberyite ($\text{MgHPO}_4 \cdot 3\text{H}_2\text{O}$),

bobierite ($Mg_3(PO_4)_2$), and struvite ($NH_4MgPO_4 \cdot 6H_2O$). Due to ivory's higher magnesium content, DAP consolidation will assuredly run into the same issues of magnesium phosphate formation as found in the experimental bone consolidations. Even immersing ivory in ammoniated solutions (an old conservation treatment) produced well-defined struvite crystals (Freund et al. 2002). It is possible that magnesium phosphate crystals would result in a successful consolidation, but those results, and the use of DAP as a consolidant for ivory would need further study.

8.1.3 Effects on paleodietary and other analyses

Generally speaking, the elements used for paleodietary analyses are those, which are not affected by diagenetic alterations, which would make drawing conclusions about pre-mortem behaviors problematic. Studies on strontium found in bone have been used for paleodietary research since the 1950s. Strontium is not affected by diagenetic processes, as it enters the bone as a substitute for calcium within the apatite crystal matrix. Strontium concentrations can differentiate between plant- or animal-based diets, the shift from hunting-gathering to agriculture, and coastal and inland food sources. Additional elements used for paleodietary analyses are zinc, manganese, copper, and vanadium (Runia 1987). These elements do not substitute in the HAP structure, and so treatment with DAP should not affect subsequent analysis. However, more study is needed to confirm that this is so.

8.1.4 Additional calcium sources

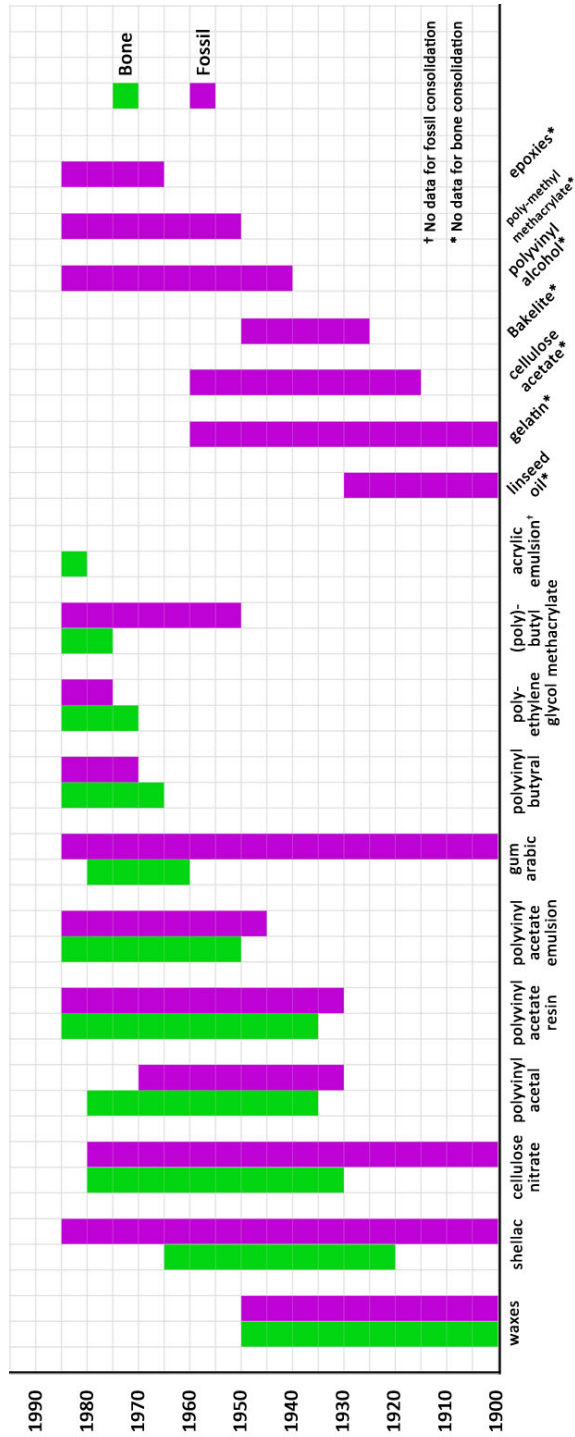
There is potential for the addition of calcium cations via calcium hydroxide solutions or nanoparticle dispersions as a preliminary step prior to the application of DAP, although whether

the reaction would still preferentially form magnesium phosphates would need to be examined. The calcium hydroxide particles fill larger gaps and cavities, and are converted to calcium carbonate. By introducing this additional calcium content, the phosphates used to form HAP now have a much richer feeding ground, and form a tightly interconnected, yet porous, structure. Severely degraded and demineralized bone may have lost a significant portion of its original calcium content, and simply introducing phosphates on their own may not be enough to create a new HAP network. If calcium can be reintroduced using calcium hydroxide, The HAP consolidation would potentially be much more successful. Laboratory tests and analysis must be performed to determine whether the high alkalinity of calcium hydroxide dispersions negatively affect the organic content in bone.

Overall, the use of biomimetic HAP is very promising as a consolidating agent for degraded bone, and one could also find successful applications for archaeological teeth, shell, and calcified tissue. The controlled application of aqueous DAP solutions, following a standardized procedure, can significantly increase the cohesiveness of friable bone material, while preserving the bone's physiochemical properties. Further study is needed to examine the reactions between the DAP solutions and the complex array of elements and compounds found within bone, but these preliminary results point towards a promising new method of archaeological conservation.

Chapter 9: Appendix

9.1 Time frame for use of various consolidants on bone and fossil, for the time period 1900-1985 (based on Howie 1984 and Johnson 1994)

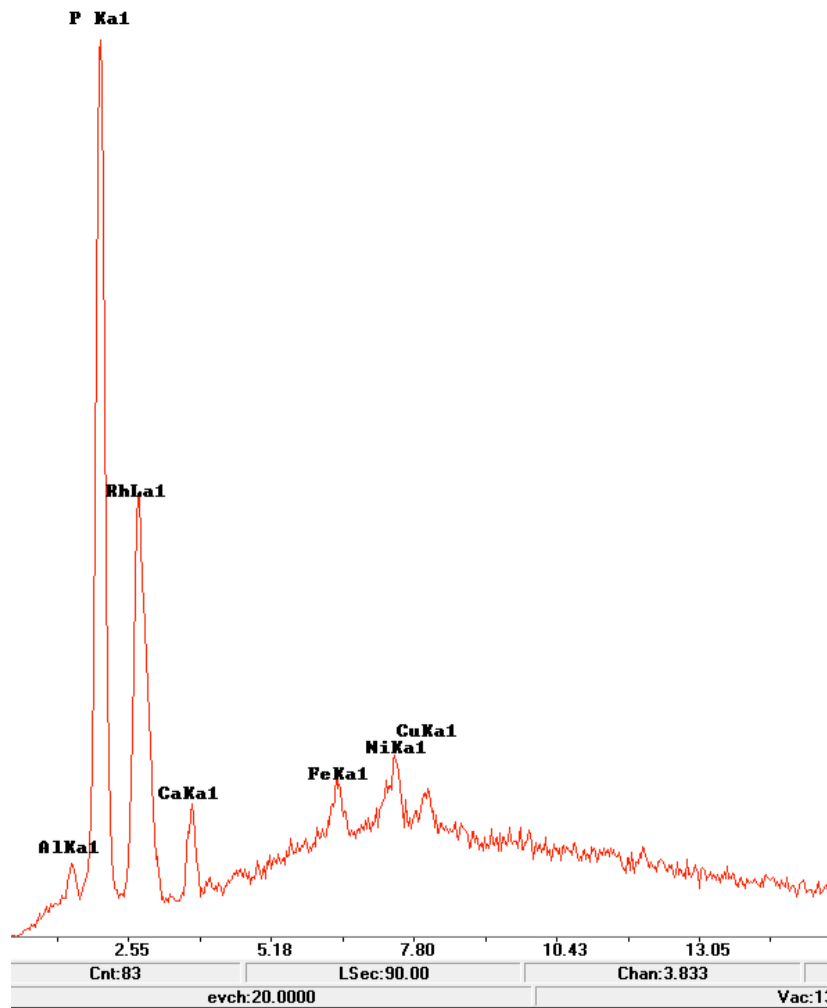


9.2 XRD spectrum of bone flour sample

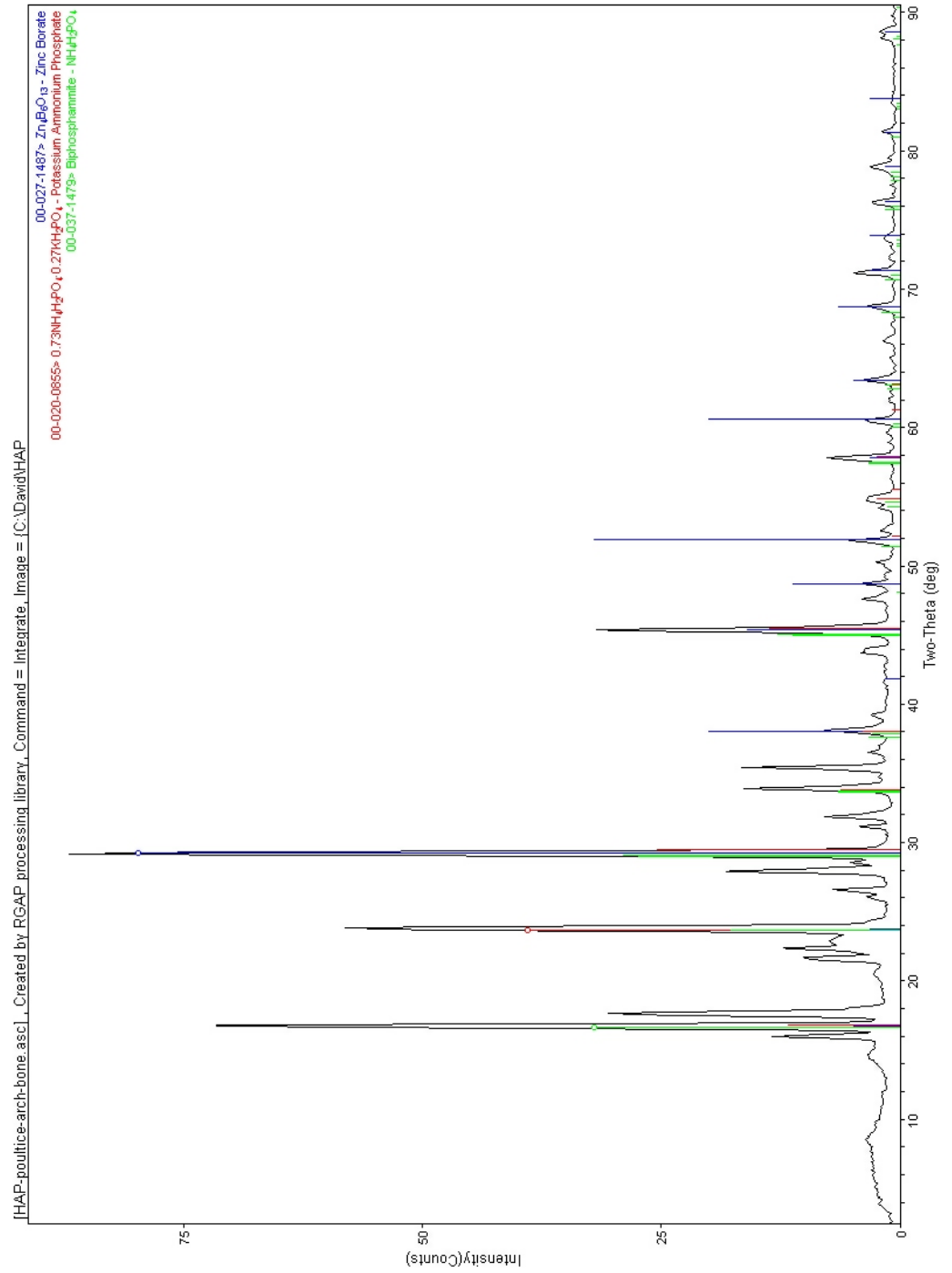


9.3 Analysis of poultice used on archaeological bone samples

9.3.1 XRF spectrum of poultice

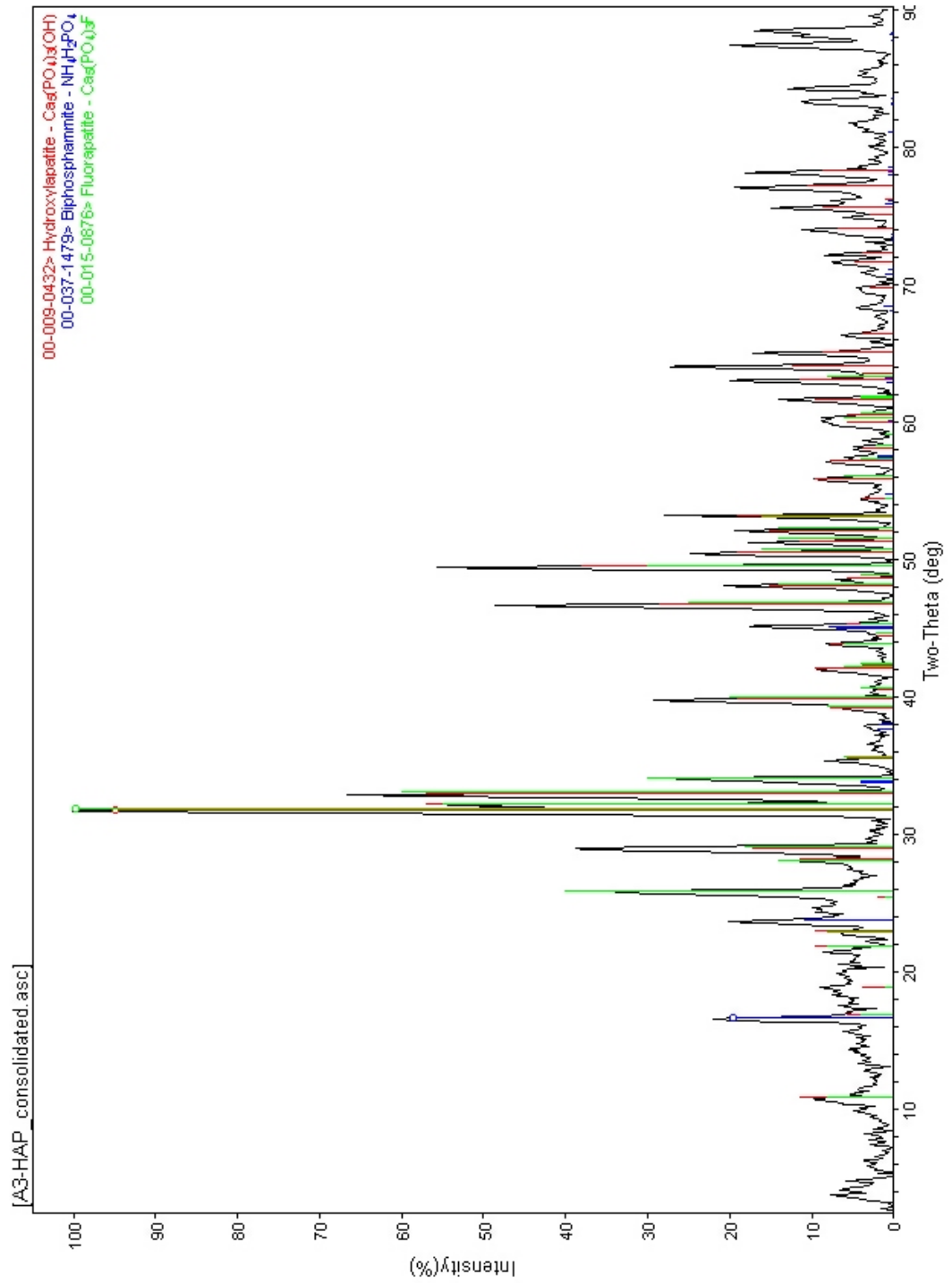


9.3.2 XRD spectrum of poulitce

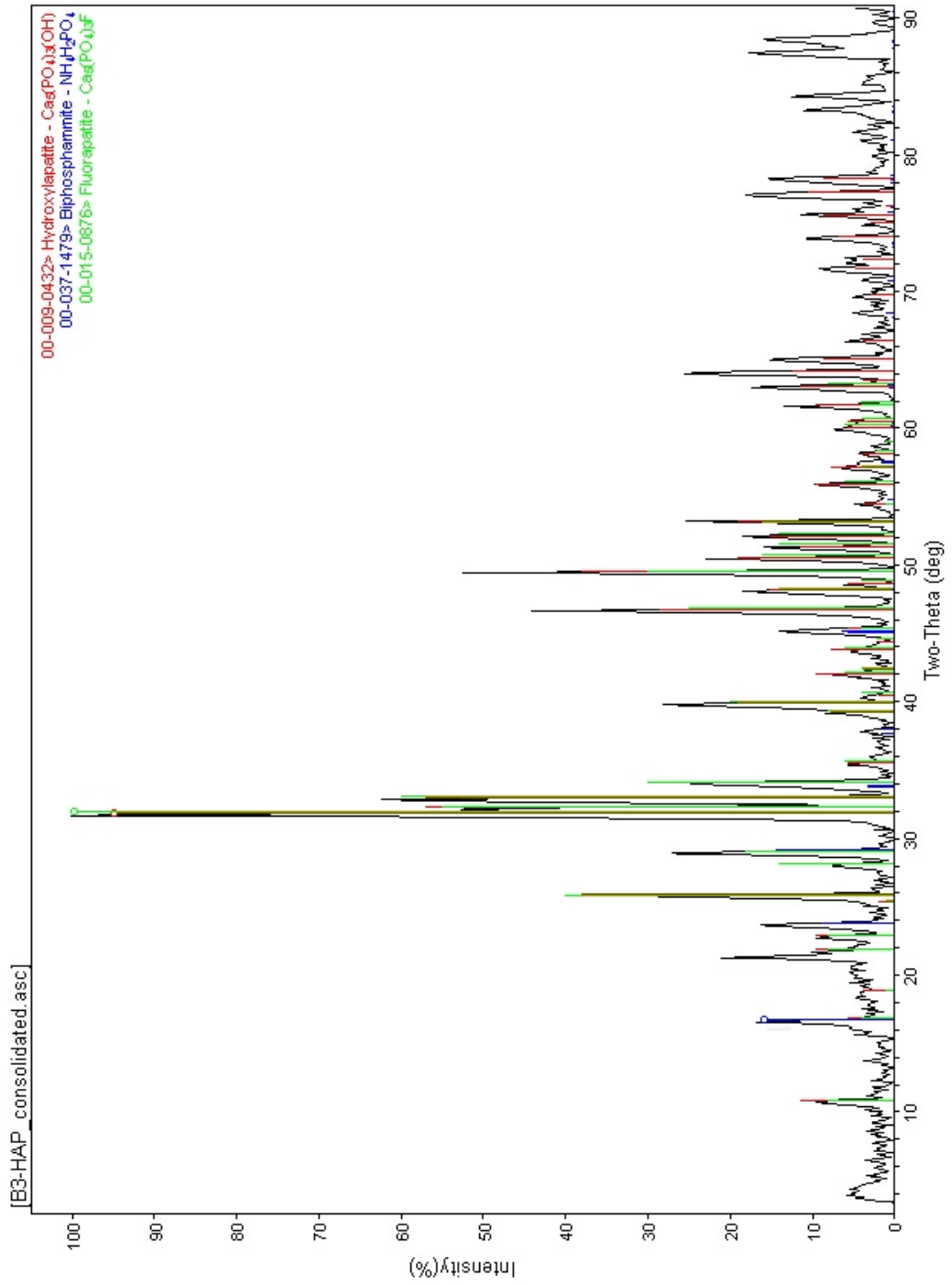


9.4 XRD spectra of bone flour samples after treatment with DAP

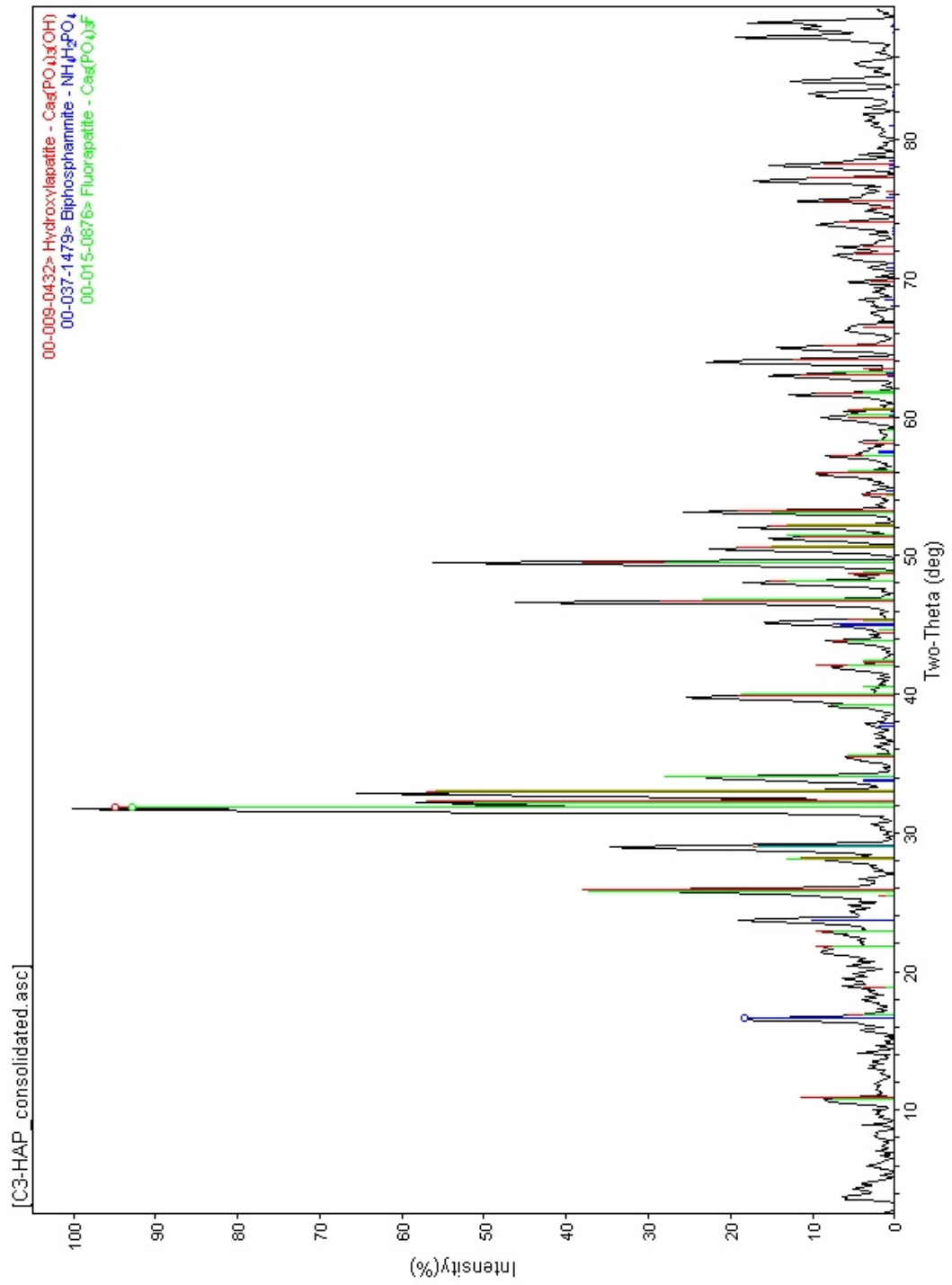
9.4.1 Sample treated with 0.5M DAP



9.4.2 Sample treated with 1.0M DAP

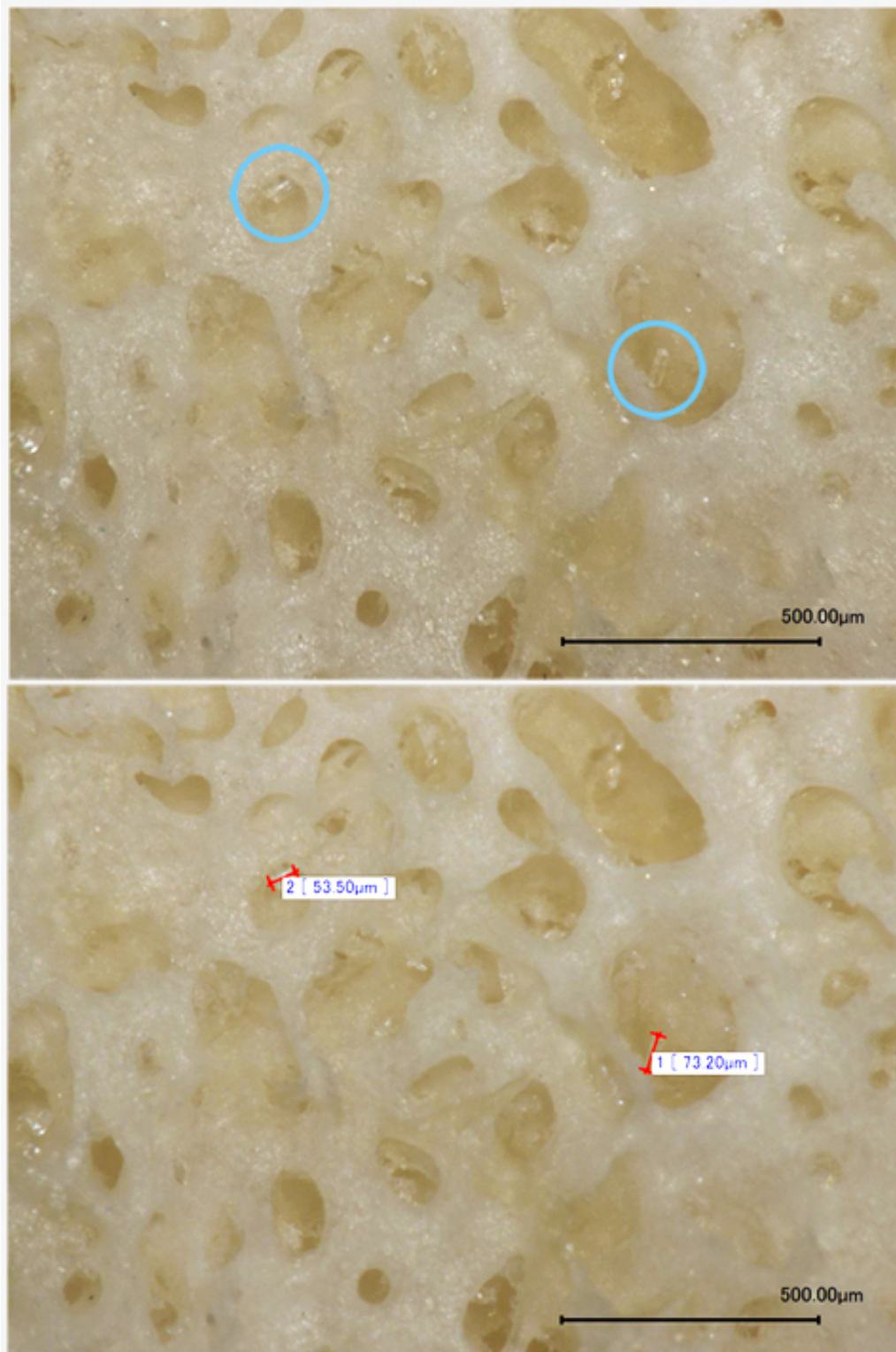


9.4.3 Sample treated with 2.0M DAP

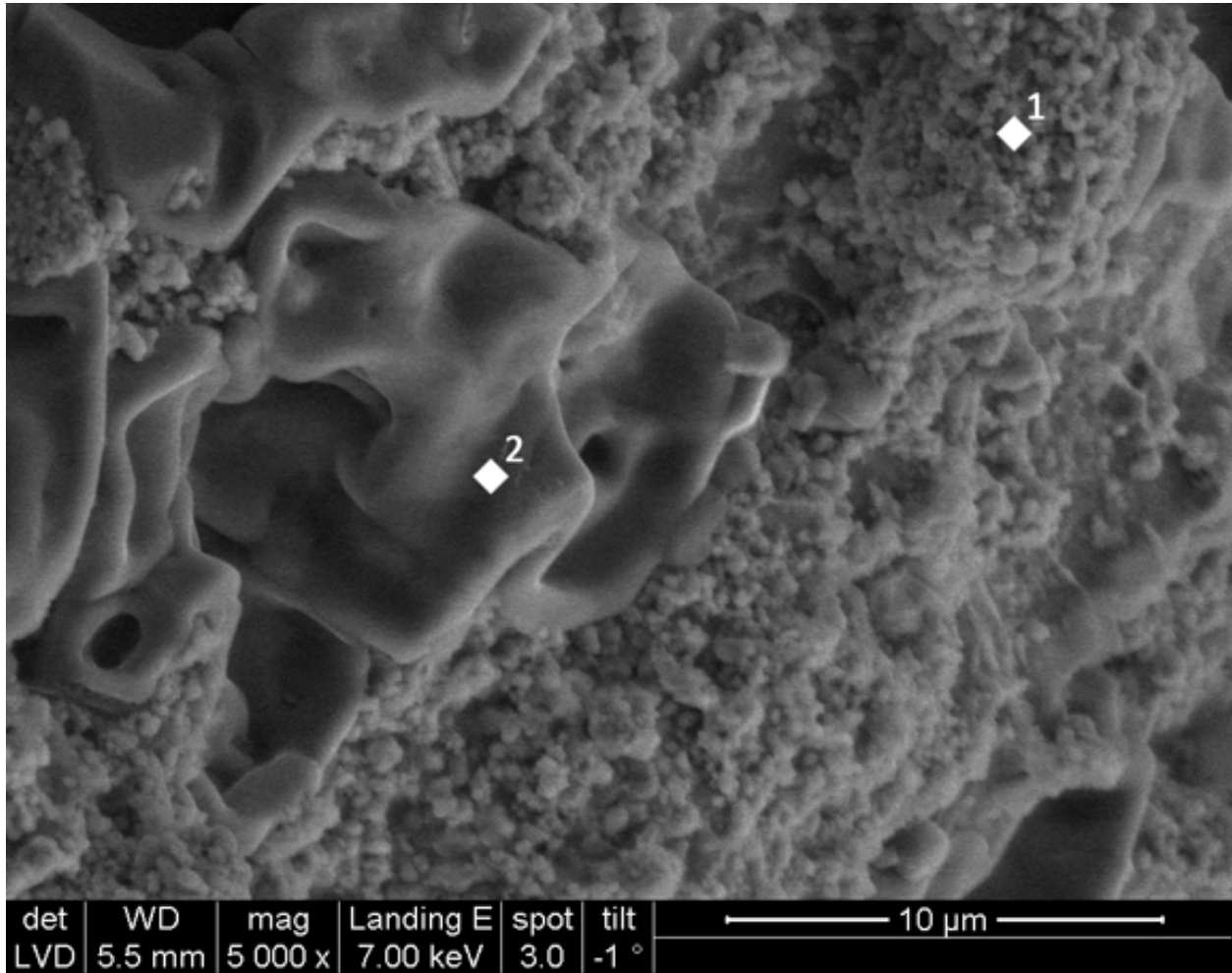


9.5 Digital Microscope photomicrographs of modern bone samples

9.5.1 DM images of modern bone treated with 1.0M DAP, revealing crystals on the surface and their largest dimension



9.6 SEM-EDS of bone flour samples



Weight %

	<i>C-K</i>	<i>N-K</i>	<i>O-K</i>	<i>Mg-K</i>	<i>Al-K</i>	<i>P-K</i>	<i>Ca-K</i>	<i>Sr-L</i>
3c(1)_pt1	1.68		39.12			21.90	37.29	
3c(1)_pt2	1.59	7.26	52.70	0.30	0.36	17.39	20.39	0.00

Weight % Error (+/- 1 Sigma)

	<i>C-K</i>	<i>N-K</i>	<i>O-K</i>	<i>Mg-K</i>	<i>Al-K</i>	<i>P-K</i>	<i>Ca-K</i>	<i>Sr-L</i>
3c(1)_pt1	+/-0.38		+/-1.03			+/-0.36	+/-0.42	
3c(1)_pt2	+/-0.38	+/-1.28	+/-0.96	+/-0.07	+/-0.06	+/-0.29	+/-0.28	+/-0.00

Atom %

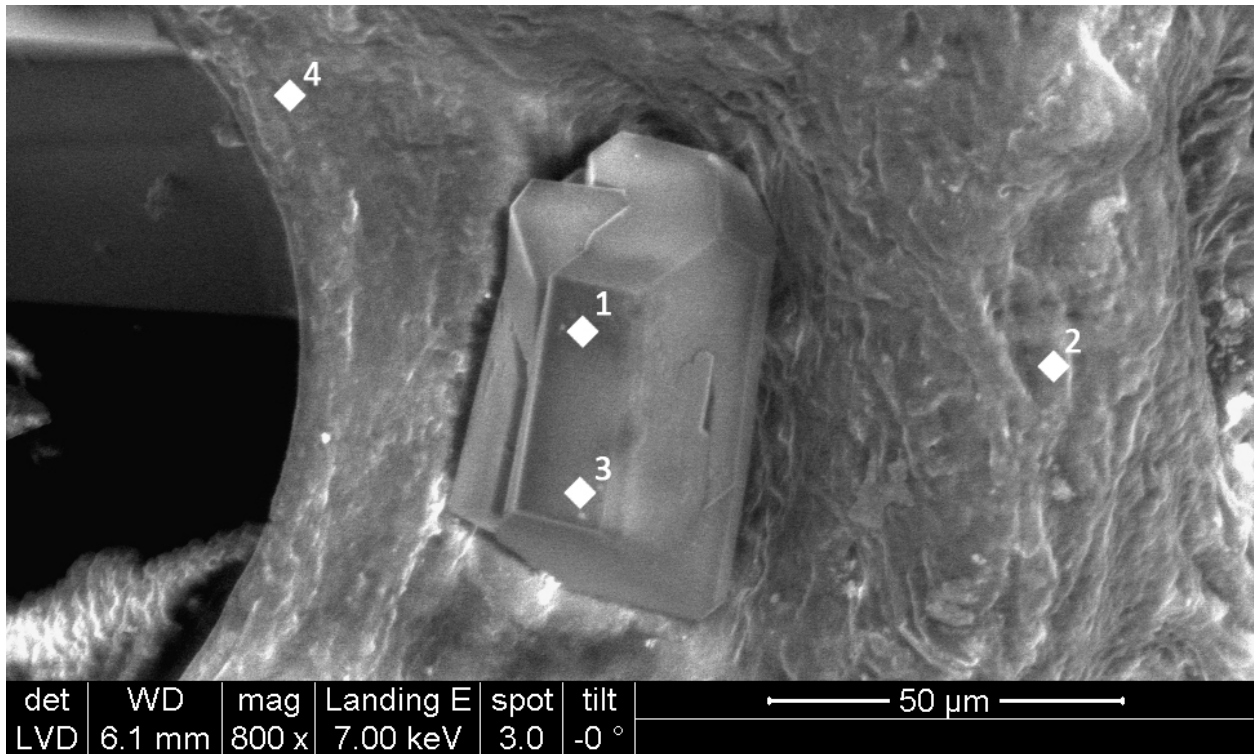
	<i>C-K</i>	<i>N-K</i>	<i>O-K</i>	<i>Mg-K</i>	<i>Al-K</i>	<i>P-K</i>	<i>Ca-K</i>	<i>Sr-L</i>
3c(1)_pt1	3.31		57.90			16.75	22.04	
3c(1)_pt2	2.62	10.29	65.35	0.24	0.26	11.14	10.09	0.00

Atom % Error (+/- 1 Sigma)

	<i>C-K</i>	<i>N-K</i>	<i>O-K</i>	<i>Mg-K</i>	<i>Al-K</i>	<i>P-K</i>	<i>Ca-K</i>	<i>Sr-L</i>
3c(1)_pt1	+/-0.75		+/-1.52			+/-0.27	+/-0.25	
3c(1)_pt2	+/-0.62	+/-1.82	+/-1.19	+/-0.05	+/-0.04	+/-0.19	+/-0.14	+/-0.00

9.7 SEM-EDS of modern bone samples

9.7.1 Sample treated with 0.5M DAP



Weight Percent:

	<i>C-K</i>	<i>O-K</i>	<i>Na-K</i>	<i>Mg-K</i>	<i>P-K</i>	<i>S-K</i>	<i>Cl-K</i>	<i>Ca-K</i>
<i>sample2B_pt1</i>	23.63	58.49		6.84	10.55			0.50
<i>sample2B_pt2</i>	67.09	26.79	0.64		2.57	1.66	0.61	0.64
<i>sample2B_pt3</i>	11.09	67.95		8.55	11.53			0.87
<i>sample2B_pt4</i>	58.70	34.98		0.38	2.67	1.27		2.00

Weight Percent Error (+/- 1 Sigma)

	<i>C-K</i>	<i>O-K</i>	<i>Na-K</i>	<i>Mg-K</i>	<i>P-K</i>	<i>S-K</i>	<i>Cl-K</i>	<i>Ca-K</i>
<i>sample2B_pt1</i>	+/-0.64	+/-0.62		+/-0.15	+/-0.21			+/-0.08
<i>sample2B_pt2</i>	+/-0.83	+/-1.14	+/-0.12		+/-0.13	+/-0.13	+/-0.11	+/-0.14
<i>sample2B_pt3</i>	+/-0.64	+/-0.56		+/-0.16	+/-0.22			+/-0.16
<i>sample2B_pt4</i>	+/-1.57	+/-1.53		+/-0.13	+/-0.25	+/-0.23		+/-0.40

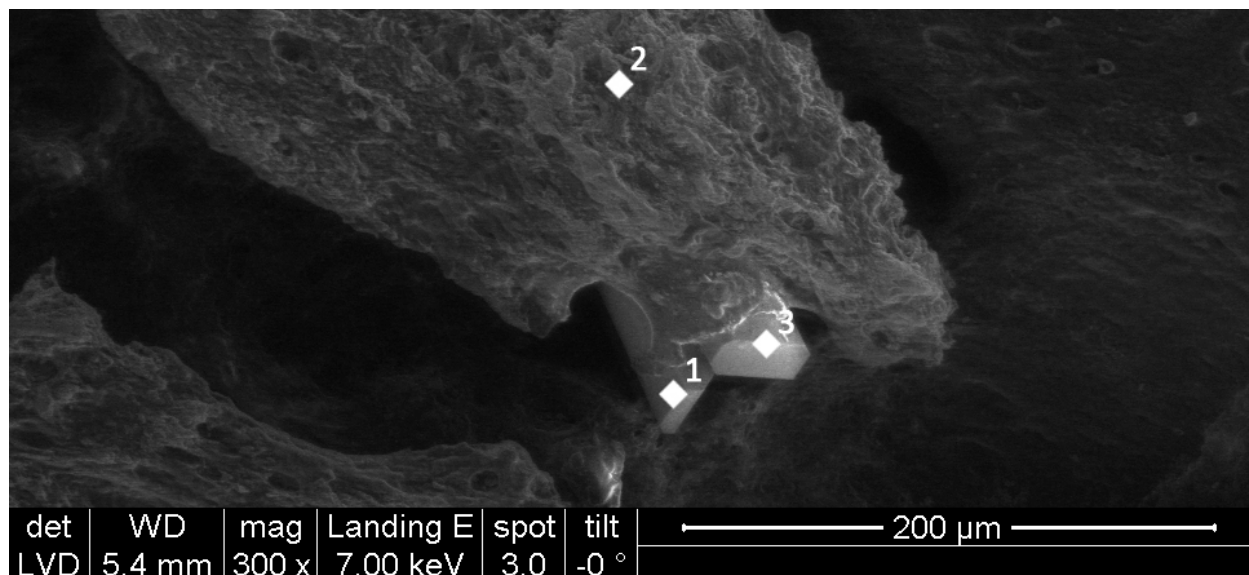
Atom Percent

	<i>C-K</i>	<i>O-K</i>	<i>Na-K</i>	<i>Mg-K</i>	<i>P-K</i>	<i>S-K</i>	<i>Cl-K</i>	<i>Ca-K</i>
<i>sample2B_pt1</i>	31.44	58.42		4.50	5.44			0.20
<i>sample2B_pt2</i>	74.92	22.46	0.37		1.11	0.69	0.23	0.21
<i>sample2B_pt3</i>	15.61	71.78		5.95	6.29			0.37
<i>sample2B_pt4</i>	67.27	30.09		0.22	1.18	0.55		0.69

Atom % Error (+/- 1 Sigma)

	<i>C-K</i>	<i>O-K</i>	<i>Na-K</i>	<i>Mg-K</i>	<i>P-K</i>	<i>S-K</i>	<i>Cl-K</i>	<i>Ca-K</i>
<i>sample2B_pt1</i>	+/-0.85	+/-0.62		+/-0.10	+/-0.11			+/-0.03
<i>sample2B_pt2</i>	+/-0.93	+/-0.96	+/-0.07		+/-0.06	+/-0.05	+/-0.04	+/-0.05
<i>sample2B_pt3</i>	+/-0.90	+/-0.59		+/-0.11	+/-0.12			+/-0.07
<i>sample2B_pt4</i>	+/-1.79	+/-1.32		+/-0.08	+/-0.11	+/-0.10		+/-0.14

9.7.2 Sample treated with 1.0M DAP



Weight Percent

	<i>C-K</i>	<i>O-K</i>	<i>Mg-K</i>	<i>P-K</i>	<i>Ca-K</i>
<i>sample2D_pt1</i>	25.44	50.10	6.03	14.20	4.23
<i>sample2D_pt2</i>	26.52	31.74	0.37	15.32	26.06
<i>sample2D_pt3</i>	20.91	58.78	5.92	11.01	3.39

Weight Percent Error (+/- 1 Sigma)

	C-K	O-K	Mg-K	P-K	Ca-K
sample2D_pt1	+/-0.76	+/-0.72	+/-0.15	+/-0.27	+/-0.29
sample2D_pt2	+/-0.52	+/-0.72	+/-0.05	+/-0.22	+/-0.27
sample2D_pt3	+/-0.60	+/-0.61	+/-0.13	+/-0.21	+/-0.21

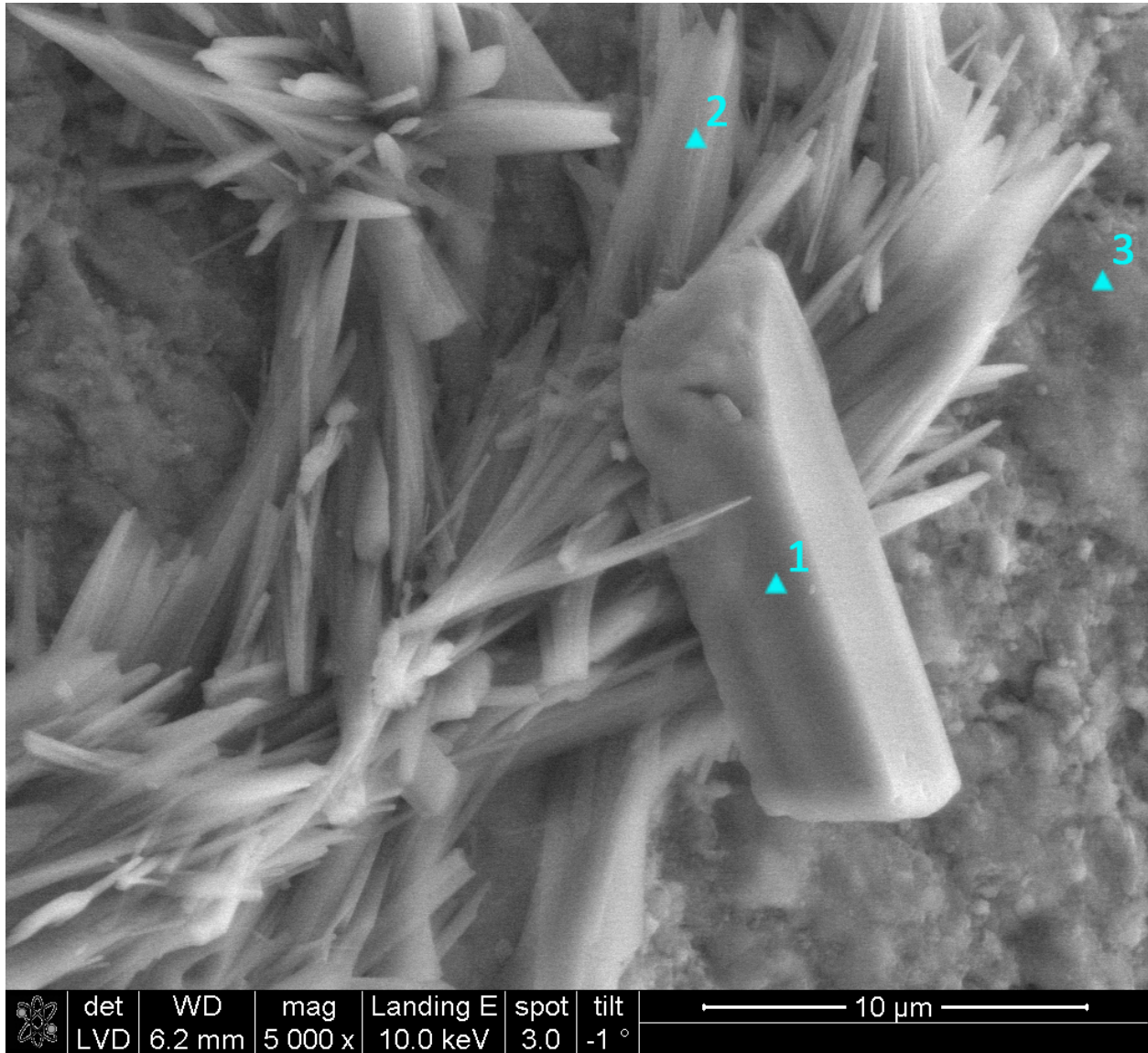
Atom Percent

	C-K	O-K	Mg-K	P-K	Ca-K
sample2D_pt1	34.94	51.66	4.10	7.56	1.74
sample2D_pt2	41.26	37.07	0.28	9.24	12.15
sample2D_pt3	28.55	60.24	3.99	5.83	1.39

Atom Percent Error (+/- 1 Sigma)

	C-K	O-K	Mg-K	P-K	Ca-K
sample2D_pt1	+/-1.05	+/-0.75	+/-0.10	+/-0.15	+/-0.12
sample2D_pt2	+/-0.80	+/-0.84	+/-0.04	+/-0.13	+/-0.13
sample2D_pt3	+/-0.82	+/-0.62	+/-0.09	+/-0.11	+/-0.09

9.8 EDS of archaeological bone samples



Weight %

	<i>C-K</i>	<i>N-K</i>	<i>O-K</i>	<i>Na-K</i>	<i>Mg-K</i>	<i>Al-K</i>	<i>P-K</i>	<i>Ca-K</i>
<i>arch1(5)_pt1</i>	5.04		66.70		5.56		14.63	7.73
<i>arch1(5)_pt2</i>	6.33	9.78	54.48			0.32	16.18	12.91
<i>arch1(5)_pt3</i>	8.92		50.31	0.69	0.48		15.05	24.55

Weight % Error (+/- 1 Sigma)

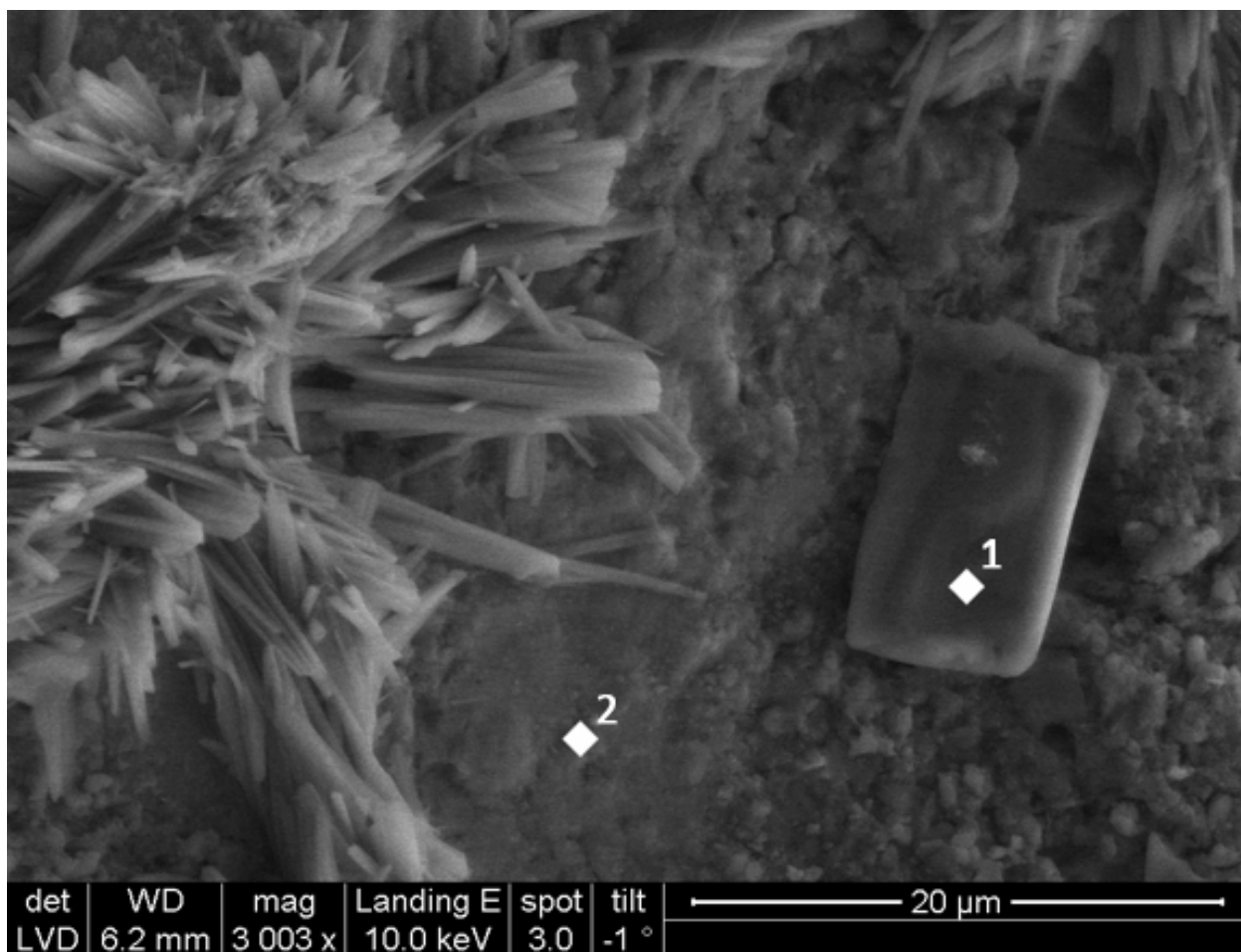
	C-K	N-K	O-K	Na-K	Mg-K	Al-K	P-K	Ca-K
arch1(5)_pt1	+/-0.94		+/-1.15		+/-0.26		+/-0.40	+/-0.40
arch1(5)_pt2	+/-0.55	+/-1.40	+/-0.98			+/-0.06	+/-0.26	+/-0.32
arch1(5)_pt3	+/-0.60		+/-0.97	+/-0.12	+/-0.07		+/-0.27	+/-0.30

Atom %

	C-K	N-K	O-K	Na-K	Mg-K	Al-K	P-K	Ca-K
arch1(5)_pt1	7.64		75.94		4.16		8.60	3.51
arch1(5)_pt2	9.61	12.72	62.06			0.22	9.52	5.87
arch1(5)_pt3	14.74		62.45	0.60	0.39		9.65	12.17

Atom % Error (+/- 1 Sigma)

	C-K	N-K	O-K	Na-K	Mg-K	Al-K	P-K	Ca-K
arch1(5)_pt1	+/-1.43		+/-1.31		+/-0.20		+/-0.24	+/-0.18
arch1(5)_pt2	+/-0.84	+/-1.82	+/-1.11			+/-0.04	+/-0.15	+/-0.14
arch1(5)_pt3	+/-0.99		+/-1.21	+/-0.11	+/-0.06		+/-0.17	+/-0.15



Weight %

	<i>C-K</i>	<i>O-K</i>	<i>Mg-K</i>	<i>P-K</i>	<i>Ca-K</i>	<i>Sr-L</i>
<i>arch1(6)_pt1</i>		66.23	6.66	16.35	10.76	0.00
<i>arch1(6)_pt2</i>	6.38	51.05	0.36	16.84	25.37	0.00

Weight % Error (+/- 1 Sigma)

	<i>C-K</i>	<i>O-K</i>	<i>Mg-K</i>	<i>P-K</i>	<i>Ca-K</i>	<i>Sr-L</i>
<i>arch1(6)_pt1</i>		+/-1.18	+/-0.20	+/-0.47	+/-0.31	+/-0.00
<i>arch1(6)_pt2</i>	+/-0.62	+/-1.01	+/-0.07	+/-0.31	+/-0.50	+/-0.00

Atom %

	<i>C-K</i>	<i>O-K</i>	<i>Mg-K</i>	<i>P-K</i>	<i>Ca-K</i>	<i>Sr-L</i>
<i>arch1(6)_pt1</i>		79.45	5.26	10.14	5.15	0.00
<i>arch1(6)_pt2</i>	10.81	64.93	0.31	11.06	12.88	0.00

Atom % Error (+/- 1 Sigma)

	<i>C-K</i>	<i>O-K</i>	<i>Mg-K</i>	<i>P-K</i>	<i>Ca-K</i>	<i>Sr-L</i>
<i>arch1(6)_pt1</i>		+/-1.42	+/-0.16	+/-0.29	+/-0.15	+/-0.00
<i>arch1(6)_pt2</i>	+/-1.04	+/-1.29	+/-0.06	+/-0.20	+/-0.25	+/-0.00

Chapter 10: References

Alkhraisat, Mohammad Hamdan, Jatsue Cabrejos-Azama, Carmen Rueda Rodríguez, Luis Blanco

Jerez, and Enrique López Cabarcos. 2013. "Magnesium Substitution in Brushite Cements."

Materials Science and Engineering: C 33 (1): 475 – 481.

doi:<http://dx.doi.org/10.1016/j.msec.2012.09.017>.

Baglioni, P., and R. Giorgi. 2006. "Soft and Hard Nanomaterials for Restoration and

Conservation of Cultural Heritage." *Soft Matter* 2 (4): 293–303.

Bailey, M.J., S. Coe, D.M. Grant, G.W. Grime, and C. Jeynes. 2009. "Accurate Determination of

the Ca:P Ratio in Rough Hydroxyapatite Samples by SEM-EDS, PIXE and RBS - a Comparative Study." *X-Ray Spectrometry* 38: 343–347.

Beevers, C. A., and D. B. McIntyre. 1946. "The Atomic Structure of Fluor-apatite and Its Relation

to That of Tooth and Bone Material." *Mineralogical Magazine* 27 (194): 254–257, Plates XVI–XVIII.

Biscula, C., L. K. Elkin, and A. Davidson. 2009. "Consolidation of Fragile Fossil Bone from Ukhaa

Tolgod, Mongolia (Late Cretaceous) with Conservare OH100." *Journal of the American Institute for Conservation* 48 (1): 37–50.

- Blumenthal, Norman C., and Aaron S. Posner. 1973. "Hydroxyapatite: Mechanism of Formation and Properties." *Calcified Tissue Research* 13: 235–243.
- Brown, P. W., and B. Constantz. 1994. *Hydroxyapatite and Related Materials*. Boca Raton: CRC Press.
- Chadefaux, C., C. Vignaud, M. Menu, and I. Reiche. 2008. "Effects and Efficiency of Consolidation Treatments on Palaeolithic Reindeer Antler. Multi-analytical Study by Means of XRD, FT-IR Microspectroscopy, SEM, TEM and μ -PIXE/PIGE Analyses." *Applied Physics A: Materials Science & Processing* 92 (1): 171–177.
- Chelazzi, D., G. Poggi, Y. Jaidar, N. Toccafondi, R. Giorgi, and P. Baglioni. 2013. "Hydroxide Nanoparticles for Cultural Heritage: Consolidation and Protection of Wall Paintings and Carbonate Materials." *Journal of Colloid and Interface Science* 392: 42–49.
- Child, A. M. 1995. "Microbial Taphonomy of Archaeological Bone." *Studies in Conservation* 40 (1): 19–30.
- Collins, M.J., C.M. Nielsen-Marsh, J. Hiller, C.I. Smith, and J.P. Roberts. 2002. "The Survival of Organic Matter in Bone: A Review." *Archae* 44 (3): 383–394.
- Dorozhkin, S. V. 2009. "Calcium Orthophosphates in Nature, Biology and Medicine." *Materials* 2 (2): 399–498. doi:10.3390/ma2020399.
- Eanes, E. D., and A. S. Posner. 1968. "Intermediate Phases in the Basic Solution Preparation of Alkaline Earth Phosphates." *Calcified Tissue Research* 2: 38–48.

- . 1970. "Structure and Chemistry of Bone Material." In *Biological Calcification: Cellular and Molecular Aspects*, 1–26. New York: Appleton-Century-Crofts, Educational Division.
- Eanes, E. D., J. D. Termine, and A. S. Posner. 1967. "Amorphous Calcium Phosphate in Skeletal Tissues." *Clinical Orthopaedics and Related Research* 53: 223–236.
- Elliott, J. C., R. M. Wilson, and S. E. P. Dowker. 2002. "Apatite Structures." *Advances in X-ray Analysis* 45: 172–181.
- Fernández-Jalvo, Y., B. Sánchez-Chillón, P. Andrews, S. Fernández-López, and L. Alcalá Martínez. 2002. "Morphological Taphonomic Transformations of Fossil Bones in Continental Environments, and Repercussions on Their Chemical Composition." *Archaeometry* 44 (3): 353–361.
- Freund, Anke, Gerhard Eggert, Hartmut Kutzke, and Bruno Barbier. 2002. "On the Occurrence of Magnesium Phosphates on Ivory." *Studies in Conservation* 47 (3): 155–160.
- Grases, F., A. Costa-Bauzá, and L. García-Ferragut. 1998. "Biopathological Crystallization: a General View About the Mechanisms of Renal Stone Formation." *Advances in Colloid and Interface Science* 74 (1–3): 169 – 194. doi:[http://dx.doi.org/10.1016/S0001-8686\(97\)00041-9](http://dx.doi.org/10.1016/S0001-8686(97)00041-9).
- Hanhoun, M., L. Montastruc, C. Azzaro-Pantel, B. Biscans, M. Frèche, and L. Pibouleau. 2011. "Temperature Impact Assessment on Struvite Solubility Product: A Thermodynamic Modeling Approach." *Biochemical Engineering Journal* 167 (1): 50–58.

- Hansen, E., E. Doehne, J. Fidler, J. Larson, B. Martin, M. Matteini, C. Rodriguez-Navarro, et al. 2003. "A Review of Selected Inorganic Consolidants and Protective Treatments for Porous Calcareous Materials." *Reviews in Conservation* 4: 13–25.
- Hedges, R.E.M. 2002. "Bone Diagenesis: An Overview of Processes." *A* 44 (3): 319–328.
- Howie, F. M. 1984. "Materials Used for Conserving Fossil Specimens Since 1930: A Review." In *Adhesives and Consolidants*, 92–97. Paris: The International Institute for Conservation of Historic and Artistic Works.
- Jans, M. M. E., H. Kars, C.M. Nielsen-Marsh, C.I. Smith, A. G. Nord, P. Arthur, and N. Earl. 2002. "In Situ Preservation of Archaeological Bone: A Histological Study Within a Multidisciplinary Approach." *Archaeometry* 44 (3): 343–352.
- Johnson, J. S. 1994. "Consolidation of Archaeological Bone: A Conservation Perspective." *Journal of Field Archaeology* 21 (2): 221–233.
- Koob, S. P. 1984. "The Consolidation of Archaeological Bone." In *Adhesives and Consolidants*, 98–102. Paris: The International Institute for Conservation of Historic and Artistic Works.
- . 1986. "The Use of Paraloid B-72 as an Adhesive: Its Application for Archaeological Ceramics and Other Materials." *Studies in Conservation* 31 (1) (February 1): 7–14.
doi:10.2307/1505954.
- Lambert, J. B., S. V. Simpson, S. G. Weiner, and J. E. Buikstra. 1985. "Induced Metal-Ion Exchange in Excavated Human Bone." *Journal of Archaeological Science* 12: 85–92.

Lee, Yoong, YeongMin Hahm, Shigeki Matsuya, Masaharu Nakagawa, and Kunio Ishikawa. 2007.

“Characterization of Macroporous Carbonate-substituted Hydroxyapatite Bodies Prepared in Different Phosphate Solutions.” *Journal of Materials Science* 42 (18): 7843–7849.

doi:10.1007/s10853-007-1629-3.

Ma, Guobin, and Xiang Yang Liu. 2009. “Hydroxyapatite: Hexagonal or Monoclinic?” *Crystal*

Growth & Design 9 (7): 2991–2994. doi:10.1021/cg900156w.

Matteini, M. 2003. “The Mineral Approach to the Conservation of Mural Paintings: Barium

Hydroxide and Artificial Oxalates.” In *Conserving the Painted Past: Developing Approaches to Walling Painting Conservation*, 110–115. London: James and James.

———. 2010. “Inorganic Treatments for Cleaning, Consolidation and Protection of Mural

Paintings: Tradition and Innovation.” *Papers Presented at Works of Art and Conservation Science Today* (November 26).

Matteini, M., S. Rescic, F. Fratini, and G. Botticelli. 2011. “Ammonium Phosphates as

Consolidating Agents for Carbonatic Stone Materials Used in Architecture and Cultural Heritage: Preliminary Research.” *International Journal of Architectural Heritage:*

Conservation, Analysis, and Restoration 5 (6): 717–736.

Mays, Simon. 2010. *The Archaeology of Human Bones*. 2nd ed. New York: Routledge, Taylor and

Francis Group.

- Moreno, E.C., T.M. Gregory, and W.E. Brown. 1968. "Preparation and Solubility of Hydroxyapatite." *Journal of Research of the National Bureau of Standards - A. Physics and Chemistry* 72A (6): 773–782.
- Nancollas, G. H., and M. S. Mohan. 1970. "The Growth of Hydroxyapatite Crystals." *Archives of Oral Biology* 15: 731–745.
- Nielsen-Marsh, C.M., and R.E.M. Hedges. 2000. "Patterns of Diagenesis in Bone I: The Effects of Site Environments." *Journal of Archaeological Science* 27 (12): 1139–1150.
- Parker, R. B., and H. Toots. 1970. "Minor Elements in Fossil Bone." *Geological Society of America Bulletin* 81: 925–932.
- . 1980. "Trace Elements in Bones as Paleobiological Indicators." In *Fossils in the Making*, 197–207. Chicago: The University of Chicago Press.
- Polikreti, K., and Yannis Maniatis. 2003. "Micromorphology, Composition and Origin of the Orange Patina on the Marble Surfaces of Propylaea (Acropolis, Athens)." *Science of the Total Environment* 308 (1-3): 111–119.
- Pollard, M. H. C. 2008. "The Chemistry of Human Bone: Diet, Nutrition, Status and Mobility." *Archaeological Chemistry* 10: 346–382.
- Posner, A. S. 1969. "Crystal Chemistry of Bone Mineral." *Physiological Reviews* 49 (4): 760–787.

- Price, T. D. 1989. "Multi-element Studies of Diagenesis in Prehistoric Bone." In *The Chemistry of Prehistoric Human Bone*, Price, T. Douglas, ed., 126–154. Cambridge: Cambridge University Press.
- Reiche, I., C. Vignaud, and M. Menu. 2002. "The Crystallinity of Ancient Bone and Dentine: New Insights By Transmission Electron Microscopy." *Archaeometry* 44 (3): 447–459.
- Rogoz, A., Z. Sawlowicz, and P. Wojtal. 2012. "Diagenetic History of Woolly Mammoth (*Mammuthus Primigenius*) Skeletal Remains from the Archaeological Site Cracow Spadzista Street (B), Southern Poland." *Palaios* 27 (8): 541–549.
- Runia, L. T. 1987. *The Chemical Analysis of Prehistoric Bones: A Paleodietary and Ecoarchaeological Study of Bronze Age West-Friesland*. BAR International Series 363. British Archaeological Reports.
- Sassoni, E., S. Naidu, and G. W. Scherer. 2011. "The Use of Hydroxyapatite as a New Inorganic Consolidant for Damaged Carbonate Stones." *Journal of Cultural Heritage* 12: 346–355.
- Serbetci, K., F. Korkusuz, and N. Hasirci. 2000. "Mechanical and Thermal Properties of Hydroxyapatite-impregnated Bone Cement." *Turkish Journal of Medical Sciences* 30: 543–549.
- Suetsugu, Yasushi, and Junzo Tanaka. 2002. "Crystal Growth and Structure Analysis of Twin-free Monoclinic Hydroxyapatite." *Journal of Materials Science: Materials in Medicine* 13 (8): 767–772. doi:10.1023/A:1016170924138.

Teutonico, J.M. 1988. *A Laboratory Manual for Architectural Conservators*. Rome: ICCROM.

<http://books.google.com/books?id=2oLyAAAACAAJ>.

Tomazic, B., M. Tomson, and G. H. Nancollas. 1975. "Growth of Calcium Phosphates on Hydroxyapatite Crystals: The Effect of Magnesium." *Archives of Oral Biology* 20: 803–808.

Warren, J. 1999. *Conservation of Earth Structures*. Oxford: Butterworth-Heinemann.

Wilson, R. M., J. C. Elliott, and S. E. P. Dowker. 1999. "Rietveld Refinement of the Crystallographic Structure of Human Dental Enamel Apatites." *American Mineralogist* 84: 1406–1414.

Yang, F., B. Zhang, Y. Liu, G. Wei, H. Zhang, W. Chen, and Z. Xu. 2011. "Biomimic Conservation of Weathered Calcareous Stones by Apatite." *New Journal of Chemistry* 35: 887–892.